Flow regime observations in a vertical evaporator tube

Citation for published version (APA):
Geld, van der, C. W. M., & van Koppen, C. W. J. (1985). *Flow regime observations in a vertical evaporator tube*. (Report WOP-WET; Vol. 85.032). Technische Hogeschool Eindhoven.

Document status and date:
Published: 01/01/1985

Document Version:
Publisher's PDF, also known as Version of Record (includes final page, issue and volume numbers)

Please check the document version of this publication:

• A submitted manuscript is the version of the article upon submission and before peer-review. There can be important differences between the submitted version and the official published version of record. People interested in the research are advised to contact the author for the final version of the publication, or visit the DOI to the publisher's website.
• The final author version and the galley proof are versions of the publication after peer review.
• The final published version features the final layout of the paper including the volume, issue and page numbers.

Link to publication

General rights
Copyright and moral rights for the publications made accessible in the public portal are retained by the authors and/or other copyright owners and it is a condition of accessing publications that users recognise and abide by the legal requirements associated with these rights.

• Users may download and print one copy of any publication from the public portal for the purpose of private study or research.
• You may not further distribute the material or use it for any profit-making activity or commercial gain
• You may freely distribute the URL identifying the publication in the public portal.

If the publication is distributed under the terms of Article 25fa of the Dutch Copyright Act, indicated by the "Taverne" license above, please follow below link for the End User Agreement:

www.tue.nl/taverne

Take down policy
If you believe that this document breaches copyright please contact us at:

openaccess@tue.nl

providing details and we will investigate your claim.

Download date: 27. Apr. 2025

FLOW REGIME OBSERVATIONS IN A VERTICAL EVAPORATOR TUBE

C.W.M. van der Geld, C.W.J. van Koppen

BIBLIOTHEEK
8 511030
T.H.EINDHOVEN
BB 242 097

Eindhoven University of Technology
Report nr. WOP-WET 85.032

European Two Phase Flow Group Meeting 1985

FLOW REGIME OBSERVATIONS IN A VERTICAL EVAPORATOR TUBE

C.W.M. van der Geld ; C.W.J. van Koppen

ACKNOWLEDGMENTS

The authors express much gratitudes to :
P.G.M.T.Boot, D. van Bommel and J. Verspagen,
for acquisition, reduction, interpretation and presentation of data; and to:
K.Verbeek, L.v.d.Schoot and F.v.Veghel,
for conditioning and controlling the loop.
Also the continual and benevolent support of the Central Technological Department is gratefully acknowledged.

The study has been supported by the Netherlands Organization for the Advancement of Pure Research (Z.W.O.).

1 INTRODUCTION

Improved knowledge about the flow regimes occurring in two phase flows is important for a more accurate prediction of pressure drop and heat transfer. Progress in the field depends critically on a clear and objective definition of the various regimes and on our knowledge of the conditions determining transitions.

Aiming at objective definitions, measuring equipment has been developed which connects flow regimes and transitions with certain instrumental indications in unambiguous way (see van der Geld, 1984). Reference will be made to the Flow Pattern Indicator, and to differential pressure measurements with a new oil-filled tapping lines system. Both devices have been presented at the European Two Phase Flow Group Meeting, Rome 1984. A local void probe is a pair of needles seperated by ± 0.5 mm over which a DC voltage is applied. Optical device and global void meter of the conductancy type are discussed in "Measuring techniques in gas-liquid flows", J.M.Delhaye and G.Cognet (editors). Measuring strategies have been proven to be succesful in circumstances covering a wide range of system parameters.

Particular care was given to make equipment resistant to the corrosive action of demineralized water at 270 °C and 160 bars, as used in the water-steam loop at the Eindhoven University of Technology (SAGA project). With a maximum heating power of 2 MegaWatt and a maximum flowrate of 2500 kg/m^{2}s the loop offers the opportunity to study flow pattern development in a tube with a length of ± 10 m and a inner diameter of 39 mm. Results will be discussed in this paper.

2 LOOP AND DATA-ACQUISITION SYSTEM

This section contains a brief description of loop and data-acquisition system. The loop is constructed of stainless steel and carbon steel, and has maximum operation pressure of 250 bar. Power for heating is supplied by a 2 MW electrical rectifier. Thermal energy is stored in a two-phase mixture, that is transported to condenser and subcooler by a canned rotor pump.

2.1 Loop

Main components of the loop are testsection, steamdrum, condenser, subcooler, preheater and pump. Coolant circulates through the testsection upward to the steamdrum and back to the pump, partly after condensation in the condensor (see figure 2.0). The subcooler has not been active during the testruns to be described (see figure 2.1).
Flowing coolant is partly evaporated by heat generated in the wall of the testsection (Joule's heat). Water and steam are seperated in the steamdrum, whereafter the steam continues to the condensor. The water level in the drum is measured by means of level gauges, one near the drum and one at the control panel. Condensate returns to the downcomer.

The preheater consists of two concentric stainless steel tubes. The inner tube serves as electrical heating element. A variable transductor unit supplies a maximum heating power of 500 kWatt. Heating current and the applied voltage are registrated. The flow through the inner tube is balanced to that through the annular space inbetween the two tubes by means of flow restrictions at the inlet. Protection against overheating is realised by a so-called burn-out detector, that automatically can switch off the heating power.

The condensor consists of sixteen parallel tubes, that are cooled on the outside by a secondary cooling system (see figure 2.1). Cooling capacity depends on the cooling water mass flow rate. Pressure control of the entire loop is achieved by automatic adjustment of the condensor cooling capacity. The temperature in the steamdrum is compared to a preset reference temperature by an electronical control. Mass flow rate in the secundary

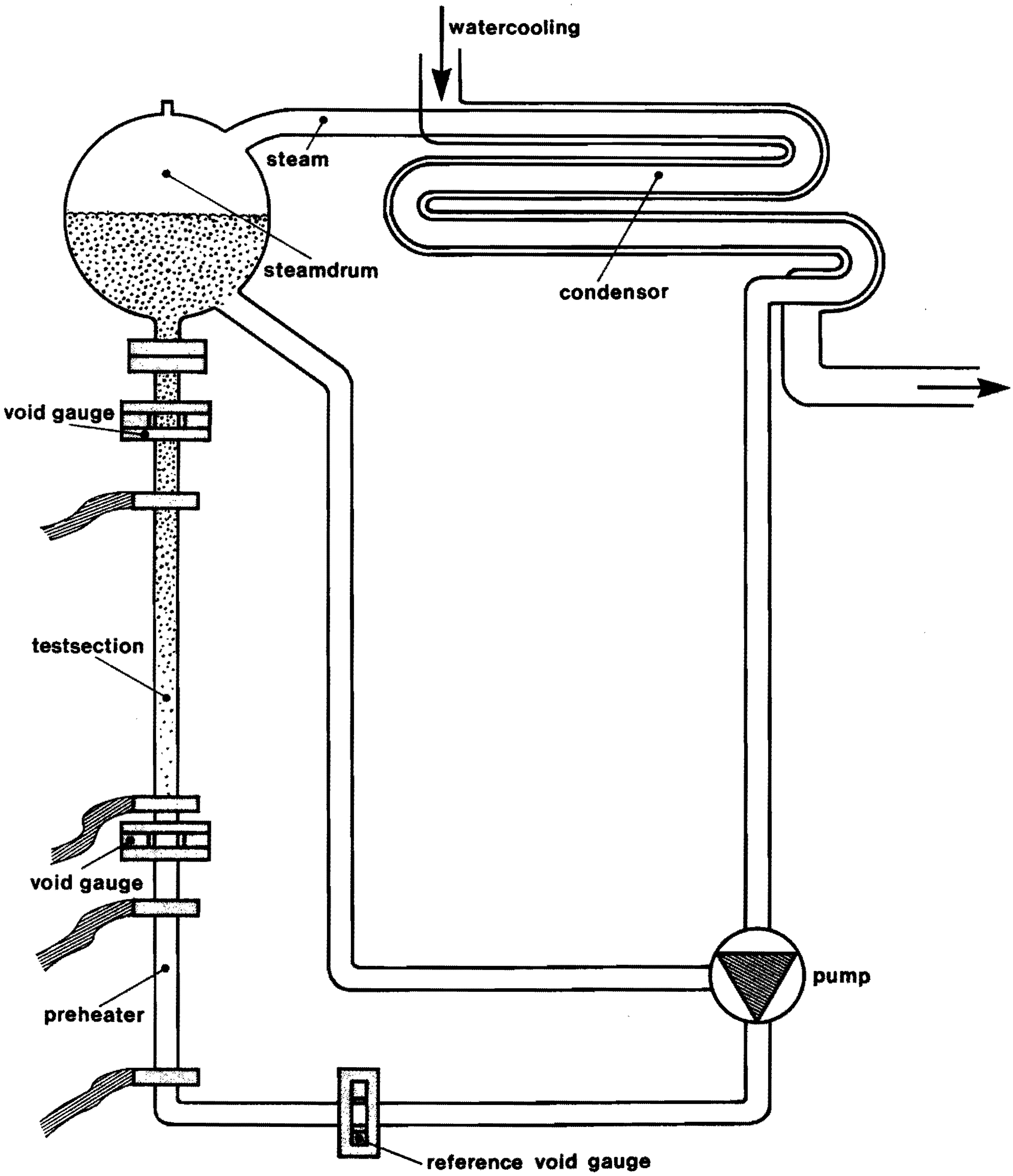

Figure 2.0

Schematics of testloop

cooling system is regulated according to the temperature deviation registred.

The water in the loop is carefully conditioned. De-airation and de-mineralisation are accomplished before operation of the loop as well as during testruns. For this purpose a bypass with high-pressure ion-filters has been installed (see figure 2.1). Salts and minerals are chemically extracted from the water. Specific electrical conductivity of the water amounts to 0.056 micro-Siemens per cm at room temperature. Heating current flowing through the water in stead of through the wall of the tessection is neglectable.

2.2 The power supply

Direct current heating power to testsection and preheater is supplied by two dual transformer/rectifier units. The maximum voltage generated is 72 Volt, and the maximum current about 7000 Ampere. After rectification a small 150 Hz component is still left (see figure 2.6). The power generated is measured in steady state operation directly with a Wattmeter. After verification with Volt- and Amperemeters the total relative error amounts to ± 0.8 %. A small error due to the electrical resistance of the electrodes and connection clamps on the testsection has been accounted for.

2.3 The test section

The testsection is a commercially available stainless steel tube. The heated length is 8.23 meters, the inner diameter 39 mm and the wall thickness 5.5 mm. Two Graylock seals embark the testsection in the loop. The tube can be installed and removed easily with the aid of a special mounting bridge. Installation or reparation of sensors can be carried out comfortably with the testsection in horizontal position.
The 150 Hz component of the power supply (see 2.2) induces currents in electronical leads. A massive carbon steel duct for electronic leads towards the central pannel minimizes these currents (Faraday's box). The part of this duct close to the testsection can be put on the mounting bridge as well.

Figure 2.1

Testloop

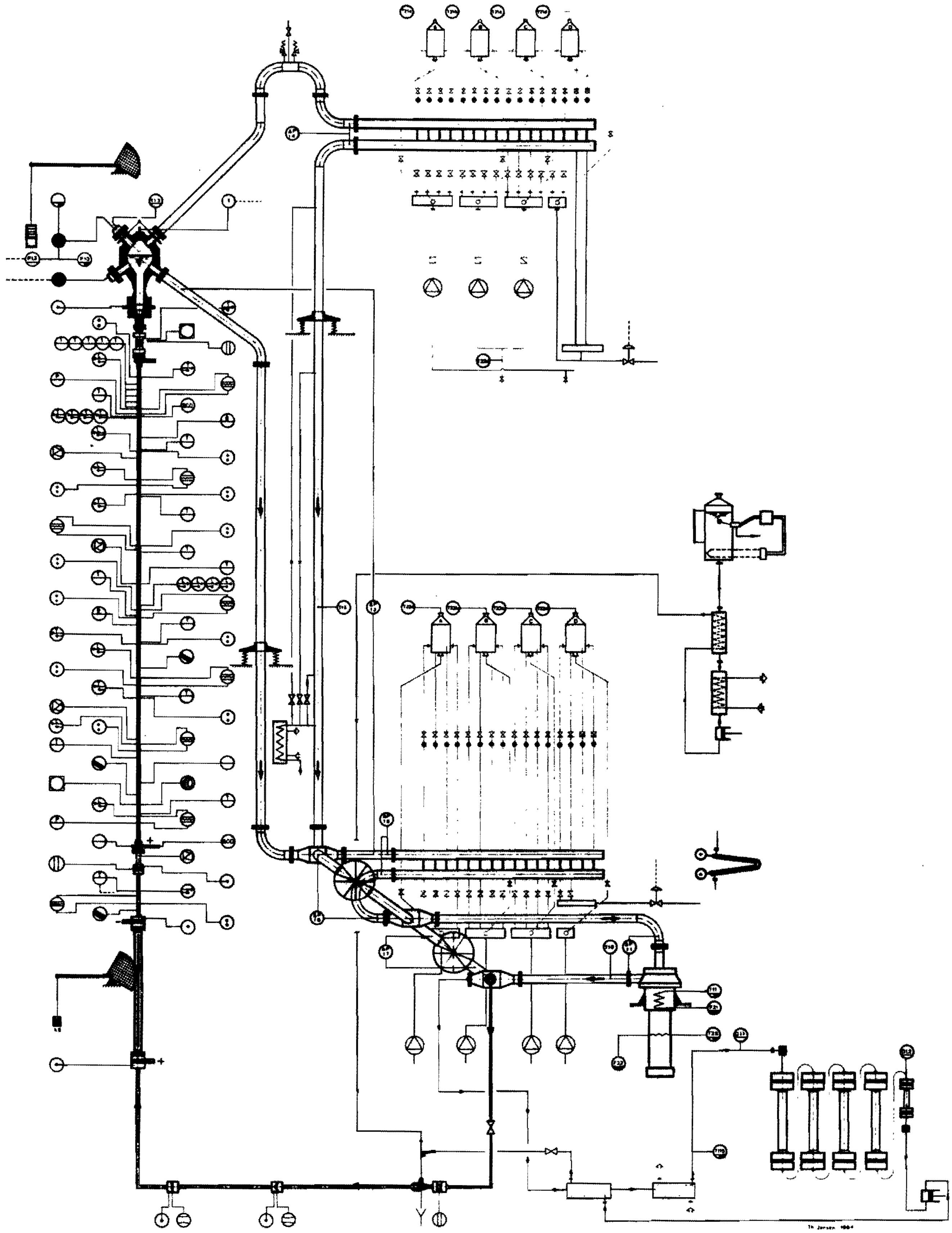

Around testsection, preheater and most other components of the loop, thermal insulation is present. Despite of this, temperature drops near the testsection indicate exterior heat losses of some 10 kW in particular circumstances. Because of corresponding temperature gradients in the tube wall, the maximum system pressure at which the testsection (and hence the loop) can be safely operated is ± 160 bar (van der Geld, 1982). Excessive temperature rise of the heated channel is prevented by means of a burn-out detector (see section 2.1).

Due to thermal expansion, the testsection length increases with some 5.6 cm during operation. Since lateral movements occur as well, flexible copper powerconnections had to be applied. A set of wheel-balances has been designed that allows for a free expansion of testsection and preheater.

Universal mounting equipment has been developed, that insulates probes from the electrically heated testsection. Most sensors can be interchanged, and mounted on several locations along testtube and calming section (see figure 2.1). A total of 80 connection points is present. More details are described in chapter 3.

Between preheater and testsection a "calming section" occurs that reduces disturbancy effects of the heating element in the preheater (see figures 2.0 and 2.1). Inlet conditions of the testsection are measured accurately in this calming section with a length of ± 2 m.

2.4 Measurement of main parameters

Main flow parameters are defined as the controlling parameters for the testloop, that are important for reproducing measurement situations and hence for making comparisons with other experiments. Heating power of testsection and preheater is measured in a way already described in 2.2. Measurement by the impedance method of the mean volume fraction of the vapor phase in inlet and outlet of the testsection will be treated in section 3.2. Calibration of these impedance gauges during testruns is realised by means of the gamma-ray technique. In principle it is possible to perform gamma-ray measurements at any location along the channel. For this purpose a table can be moved vertically along four long screwing axes. However, re-adjustment and fixation is very laborious, and the apparatus needs permanent care and control owing to its great complexity. Moreover, very long measuring periods

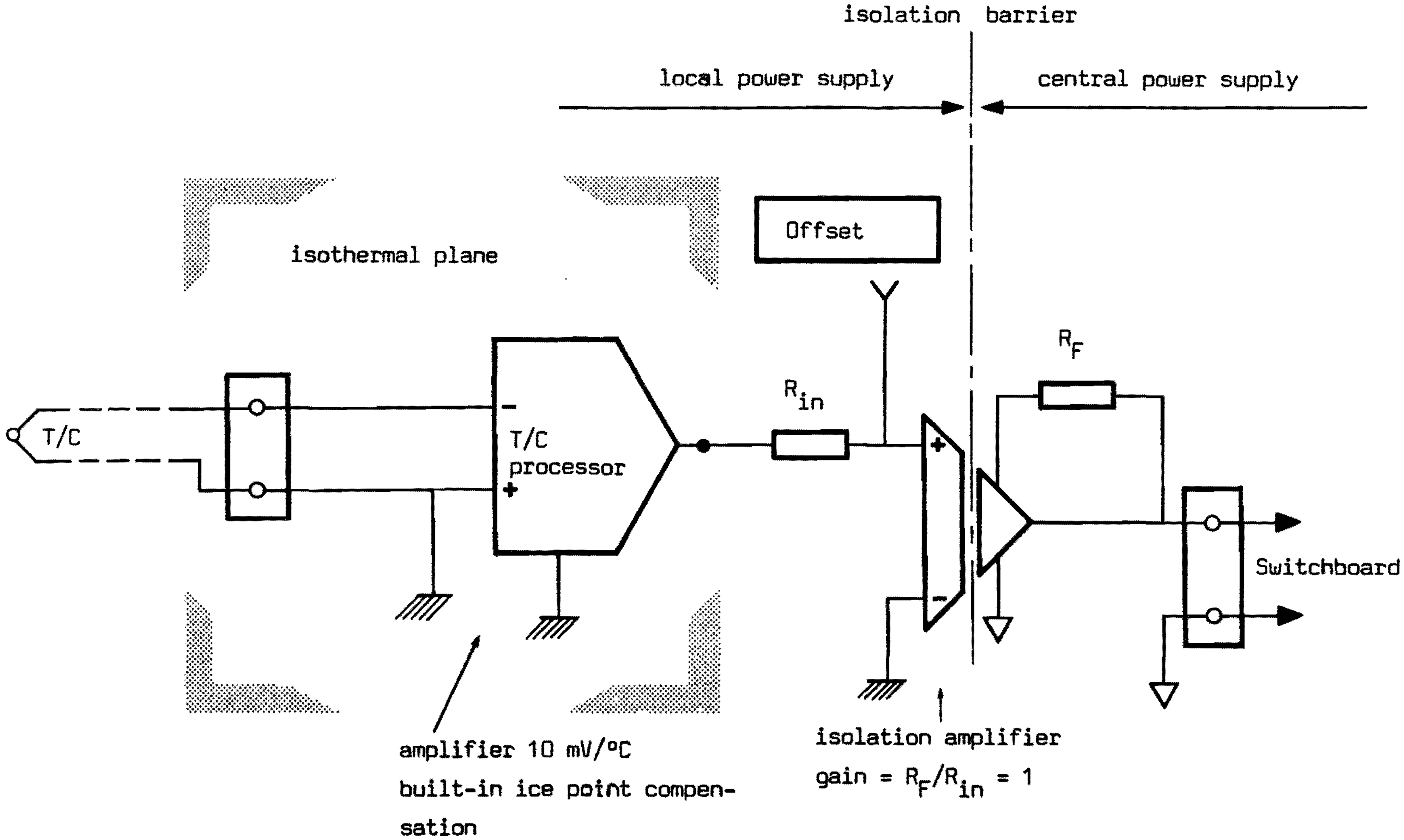

<u>Figure 2.2</u>

Thermocouple conditioner

are involved in view of the necessary counting time of pulses (see section 3.1). For these reasons, and because of the great reliability of the (theoretical) calibration curves of the overall void sensor (section 3.1), the gamma-ray technique has not been in permanent use.
Other main flow quantities will be reviewed in the current section, and are:

- system pressure
- temperature
- mass flow

2.4.1 System pressure. The absolute pressure is measured by two Bourdon type pressure gauges connected to the steamdrum. Accuracy after calibration amounts to ± 0.1 %.
Two piezo-resistive transducers can measure pressures near inlet and outlet of the testsection.

2.4.2 Temperature. Wall temperatures and temperatures of water and steam are measured with Chromel-Alumel type thermocouples, insulated by Al_2O_3 from a 0.5 mm or a 1 mm Inconel outer sheath. Wall thermocouples are fixed tightly on the tube with clamps, but are electronically insulated from it by means of 0.05 mm mica plates. Other thermocouples pass through the pressure wall by means of Conax sealings.
The thermocouples have been calibrated within an accuracy of ± 0.25 °C. Important controlling temperatures are printed continuously on a multiple pen recorder in the control panel. For these, the cold junction is furnished electronically by a Kee conditioner. For the other thermocouples, especially those in and upon the testsection, a special type of conditioner has been made (see figure 2.2). Because of the different voltage potentials induced at the locations of the sensors by the power supply, and because of the fact, that all signals are collected by the multiplexer with its own reference voltage, isolation amplifiers had to be applied. An electronical ice-point compensation makes it possible to install conditioners at locations close to the thermocouples.

2.4.3 Mass flow. The one-phase pressure drop downstream of the pump is a function of the mass velocity. Pressure drops over an orifice and a düse are measured with manometers and dynamic differential pressure transmitters (SEL

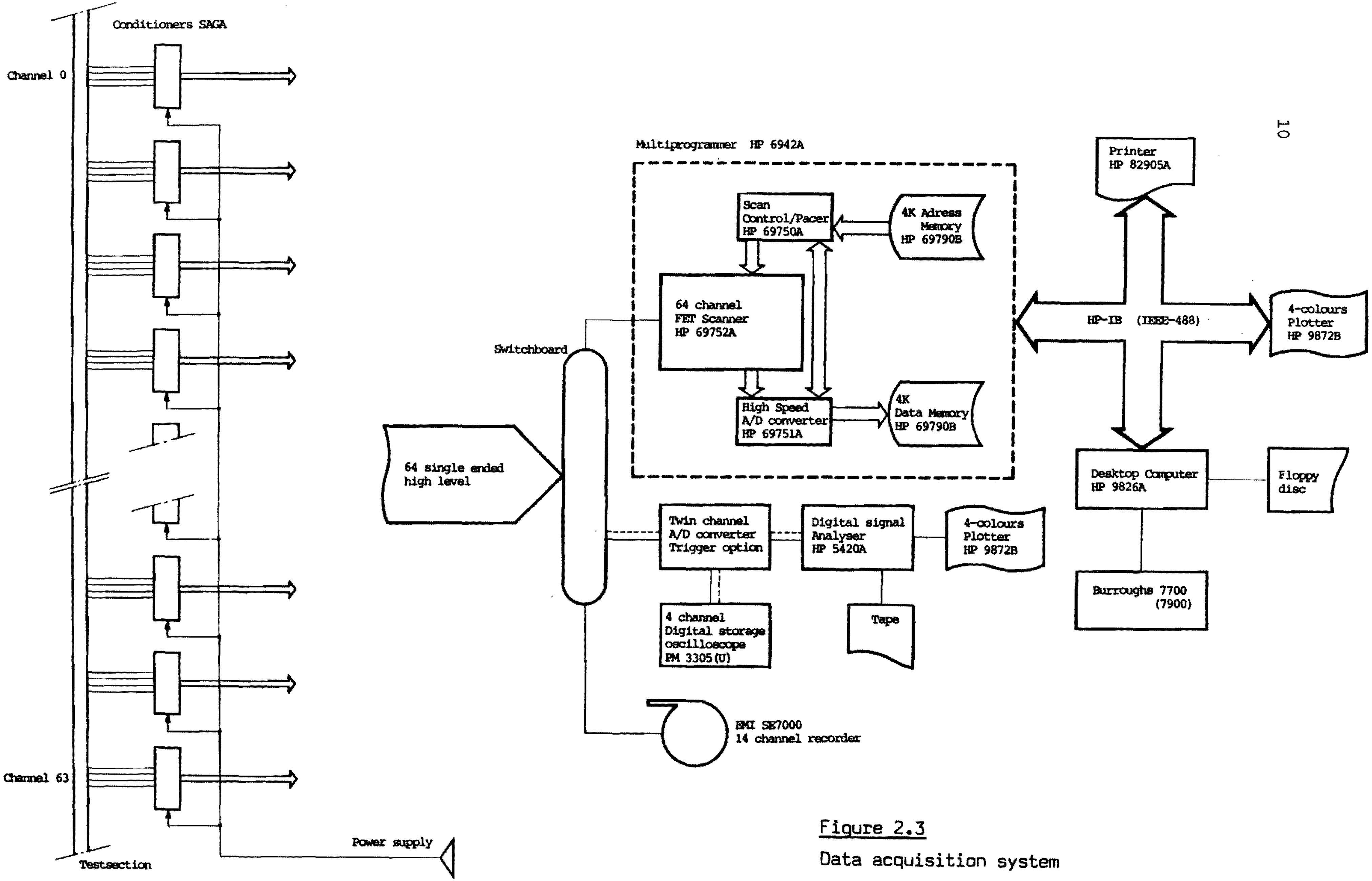

Figure 2.3

Data acquisition system

type). The manometers can be read off with an accuracy of ± 1 mm. The manometer liquids used have densities of 1750 kg/m^3, with induced accuracy of ± 8 N/m^2, and of 2950 kg/m^3. In steady state condition the transmitters have been calibrated against the manometers. The linearity is within 1 %, but gauge curves prooved to be dependent on system pressure. To detect systematic errors pressure drops of both orifice and düse are measured.
The main physical parameters of the restrictions ("k-factor") have been determined by calibration in stationary flow situation at room temperature. To calculate velocities from pressure drops, also the Reynolds number, and hence the temperature, have to be known. The latter is measured not far downstream of the restrictions. The range of Reynolds numbers where the orifice is most accurate has been chosen complementary to the range where the düse is most accurate. Signals are recorded via the multiplexer and interpreted by the computer.

2.5 Data acquisition system

The main parts and features of the data acquisition system are summarized below (see figure 2.3) :

- signal conditioners
- switchboard for 64 channels
- multiprogrammer (HP 6942A)
  - A/D converter ; maximum resolution 4.10^{-5} s
  - 12 bit ; resolution 5.10^{-5} V in the range ± 100 mV
  - 64 channel monitoring in programmable sequence
- desktop computer (HP 9826A)
  - internal disc drive (programs)
  - external disc drive (quasi-simultanous data storage)
  - graphical display (monitoring)
  - plotting capability
- magnetic tape recorder (EMI SE7000)
  - ten channels parallel (simultaneous data storage)
  - 80 kHz maximum per channel
- digital signal analyzer (HP 5420A)
  - tape cartridge (data storage)
  - band selectable analyses and power calculation

  - A/D convertors ; resolution 10^{-5} s
  - delay triggering and plotting capability
- memory oscilloscope (PM3305MC)
  - two channel mode ; programmable
  - plotting capability
- multiple colour plotter (HP9872B) and printer (HP82905A)

On-line connection to the Burrough B7900 central computer for data transfer at a rate of 2400 baut is in preparation.

The signal conditioners have been especially designed for corresponding probes. Outputs are single-ended with a range of -10 to 10 Volt to allow for undistorted transportation of signals over long distances (typically ± 20 meters). Using experimental findings of many testruns, conditioners have been optimised to yield the best possible information. Details will be discussed in the next chapter.
With the switchboard (groups of) instruments can be connected fast to taperecorder and/or signal analyzer and/or memory scope and/or multiprogrammer, in arbitrary sequence.
During the testruns to be described, the tape recorder has been used mainly for measurement of 8 differential pressure signals, simultaneous with Flow Pattern Registrations by the multiprogrammer. Also the analyzer has been used for transient data recording, but mainly for on-line and off-line frequency analyses of differential pressure signals.
Direct signal analysis and data validation is achieved by monitoring, either via the scope connected to the computer or directly on screen or plotter. The latter option is used for data validation after storage in complex sequences on floppy disk.
The main data flow line runs via switchboard and multiprogrammer to computer and disk drives. Scanning sequence and observation intervals are stored into the multiprogrammer by the computer. In each measurement, a total of 8 kbyte of data (8 bit) is received by the multiprogrammer, and send to the computer for storage on floppy disk, if necessary after data validation and/or reduction.
Local void probes are twin probes actually. To measure velocities by time-of-flight method alternate sampling is required of two signals. Maximum

sampling rate of the multiprogrammer is 25 kHz. By Shannon criteria, the physical sampling rate of each of those two channels amounts to 2.5 kHz. This resolution is high enough in many practical circumstances. Off-line analyses usually encompass validation of data and calculation of local void fraction (see figure 2.6), local velocities and flow regimes.

The combination multiprogrammer-computer offers the opportunity to register about 60 signals quasi-simultaneously. Different "scenario's", sampling sequences, are pre-programmed and loaded quickly from disk. For example, with the "overall-scenario" all the main parameters are measured (see section 2.4). Other scenario's are dedicated to Flow Pattern Indicators and Local Void Probes mainly.

3 EXPERIMENTAL RESULTS

3.1 General procedure

A summary is given of actions preceding and during measurements.
With a constant water level in the steamdrum, to achieve good seperation of water and steam, and at low power level, to prevent extreme material stresses, the system was allowed to reach desired working conditions, as quantified by the main parameters (i.e. mass flow rate, pressure, heating powers, subcooling, see section 2.4). To reduce starting-up time, the loop was kept conditioned overnights.
Only steady state measurements were performed. Signals were recorded on disk in sequences indicated by "scenario's" (see section 2.5), and simultaneously on taperecorder and analyzer. The sequential order is:

- main parameters (overall-scenario)
- temperatures on the wall
- Flow Pattern Indicators 3x
  differential pressure signals (on tape) 3x
- local void probes 3x
- temperatures on the wall
- overall-scenario (to check stationarity)

After several days, each steady state condition was repeated to check reproducibility of results.
Only signal interpretations are reproduced of those sensors, that were well-functioning during all testruns at a certain system pressure. Each Flow Pattern Indicator produces two signals, but in some cases only one signal turned out to be reliable. The good signal put forward strong indications about the flow regime present, and was used to check predictions of other instruments. Occasionally results of partly functioning instrumenst are represented, but only in the general terms "bubble", "intermittend" (designating plug or churn flow); "froth" flow.
In the appendix a complete glossary of terms is given, appropriate for measurements with Flow Pattern Indicator and differential pressure detecting system. Recordings of these instruments have been analyzed with the aid of computer programs that are based on several hundreds of measurements performed in adiabatic low-pressure loops (see Van der Geld, 1984). For ease

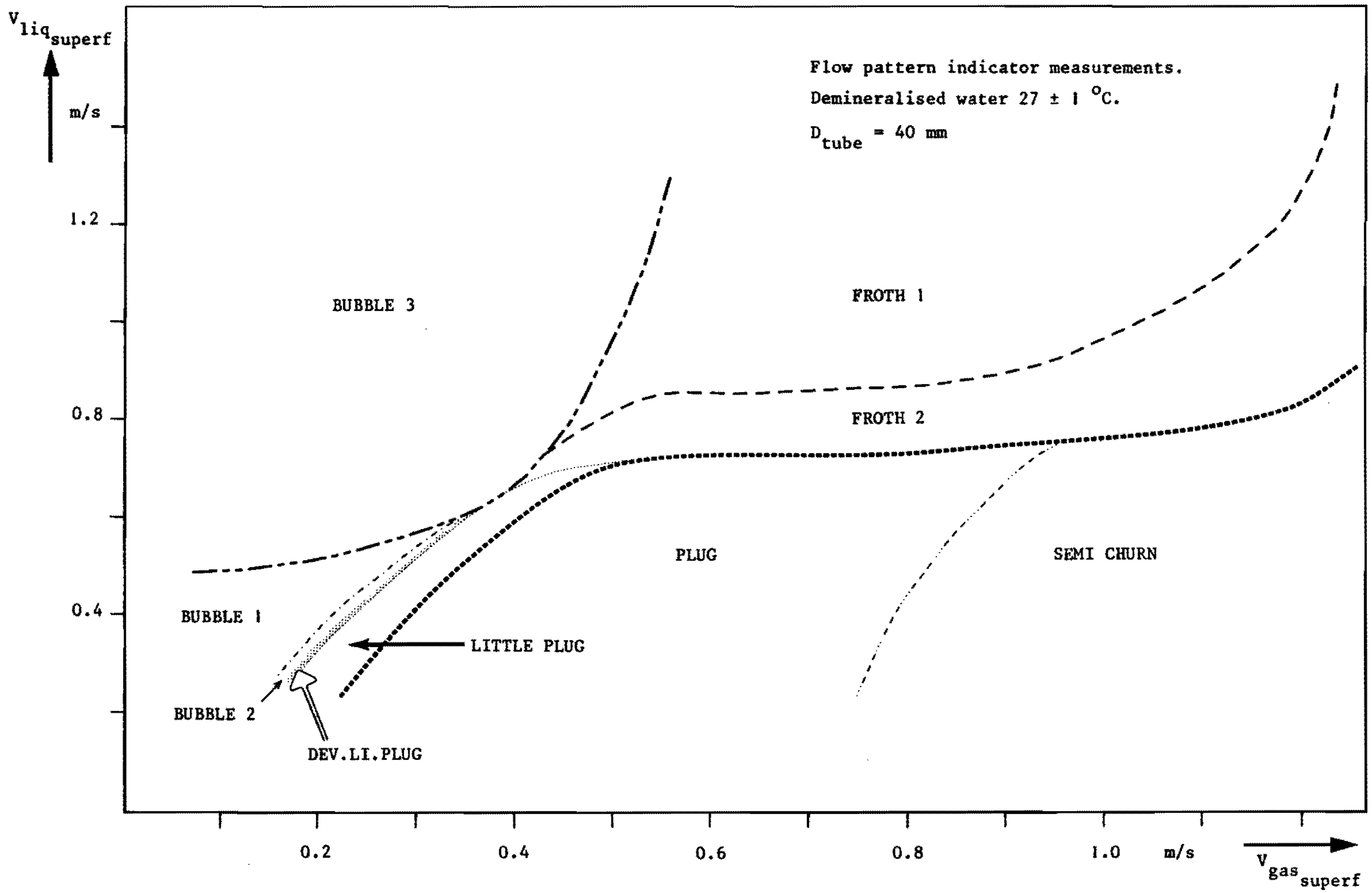

Figure 2.4

Air-water low temperature flow pattern map of reference, two flow pattern maps are reproduced (see figure 2.4 and 2.5), both for adiabatic flows and a tube diameter of 39 mm. Figure 2.4 corresponds to a standard air-water system at (nearby) room temperature. Figure 2.5 corresponds to a system of air and a binary liquid of water and ethanol, simulating the reduction of surface tension of a standard air-water system at higher temperatures. A rather drastic change of flow pattern delineation is observed. An intermittend type of flow with resemblances to plug flow, but less structured, was even undetectable with the prescribed and well-defined conditions based on the air-water observations. This plug-like flow was named "plug3", and has been re-encountered at high temperature measurements, as shall be discussed. Clearly flow regimes occurring in high-temperature water-vapor systems are simulated best by binary-liquid-air systems.

Steady state operating limits are determined mainly by safety considerations and the effects of mass flow oscillations and inhomogeneous heating. With the present configuration the lowest mass flow rate, that could be applied safely in combination with high heating powers, amounts to 800 kg/m^2s.
Maximum heating power on testsection as well as preheater is ± 250 kW.
Figures 2.4 and 2.5 show interesting steady state conditions at low superficial water velocities. The operating limits unfortunately reduce the possibilities of reaching and studying these interesting conditions at high pressures too.

3.2 Measurement strategy

Theory shows the importance of gaining better knowledge and understanding of entrance and stabilisation phenomena. For this reason it has been tried to seperate purely hydrodynamical (entrance) phenomena from other (heating) effects.
To this aim, heating power on the testsection has been adjusted such, that condensation was balanced and inlet and outlet void were approximately equal. By increasing the heating power on the preheater, subsequently different flow regimes were created in the testsection. In this way, entrance phenomena and flow development were studied in a tube with a total length of ± 10 m, in which the calming section (section 2.3) has been

Figure 2.5

Air-water-alcohol low temperature flow pattern map

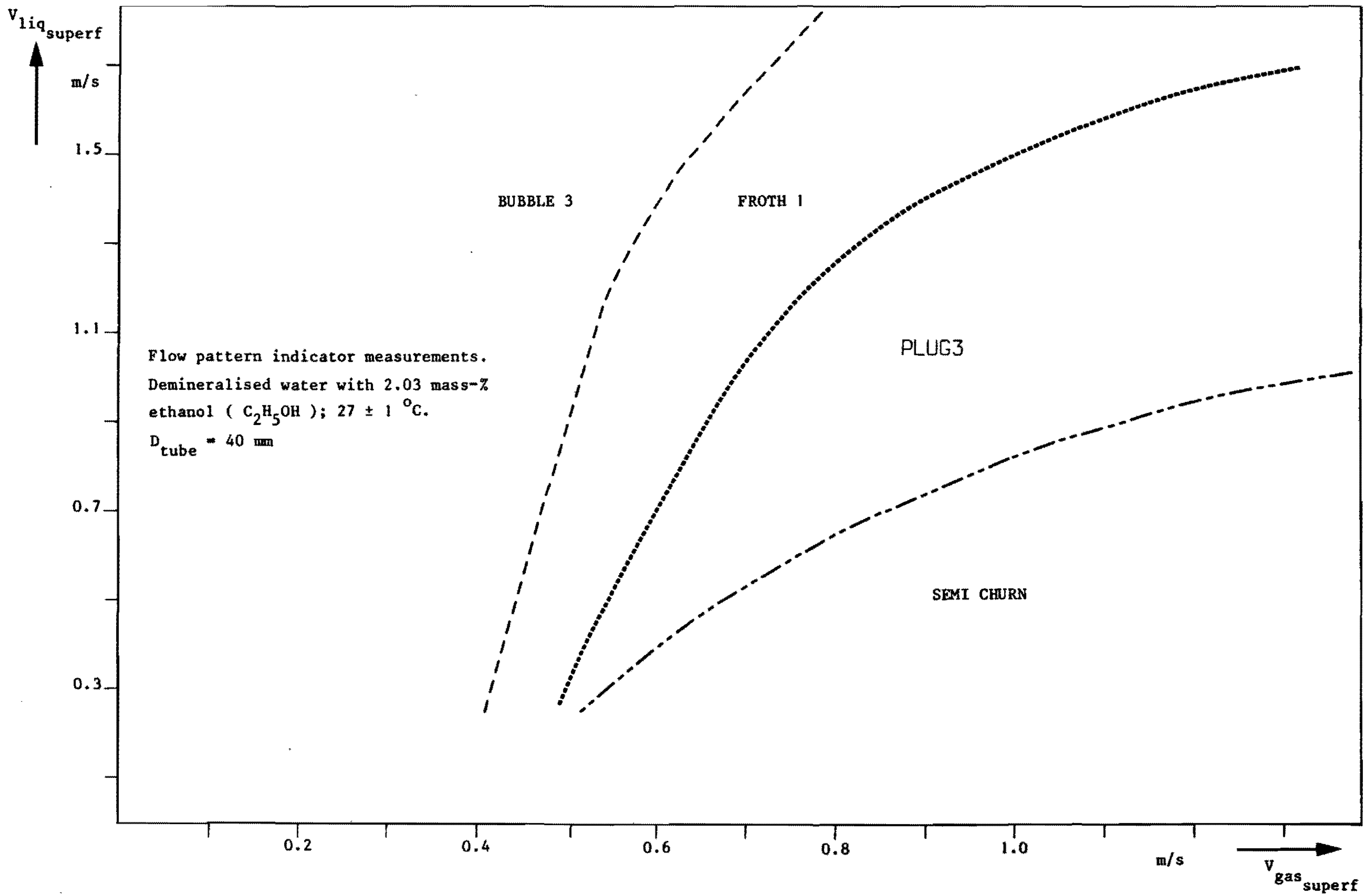

included. This measuring strategy will be referred to as "strategy-1" henceforth.

Other measurements exhibit a more phenomenological character. It has been tried to observe trends in flow regime development at large heating powers, and to check criteria based on low pressure measurements. Because of the imposed operating limits (section 3.1) no attempt has been made to study annular or whispy-annular (see Bennett et al., 1965) flows.

Mass flow rate has been varied from 800 to 2000 kg/m^{2}s, and system pressures have been studied in the range from 29 to 50 bar.

3.3 Presentation of results

Results are presented in the figures at the end of this paper. On the left hand side of these figures schematics of calming section (from 0 to - 1.2 m) and testsection, as well as physical locations of the active sensors have been designated.

Under the heading "predictions-1" predictions of the Griffith and Wallis (1961) flow pattern map occur. Interpretation of results obtained with local void probes (L.V.P. and S.V.P., see also figure 2.6) is work in progress. Photographical observations at locations near T6 and T2 were difficult to interpret, and could only confirm the results obtained with other equipment. Main parameters (see section 2.4) are presented in the block on the lower side of the figures.

Flow Pattern Indicator and differential pressure measurements with oil-filled tapping lines system are discussed in previous sections and by Van der Geld (1984).

3.4 Discussion of results

Results obtained with strategy-1 (section 3.2) are presented in for example figures 3.1 through to 3.4. The effect of increasing the mass flow rate (figures 3.1 and 3.2) is a change from bubble flow to froth flow, as was expected on grounds of figures 2.4 and 2.5.

Intermittend flows were found to occur not only with high heating powers (e.g. figures 3.3 through to 3.5), but also at higher mass flow rates with relatively low heating powers (e.g. figure 3.2). This can only be the result

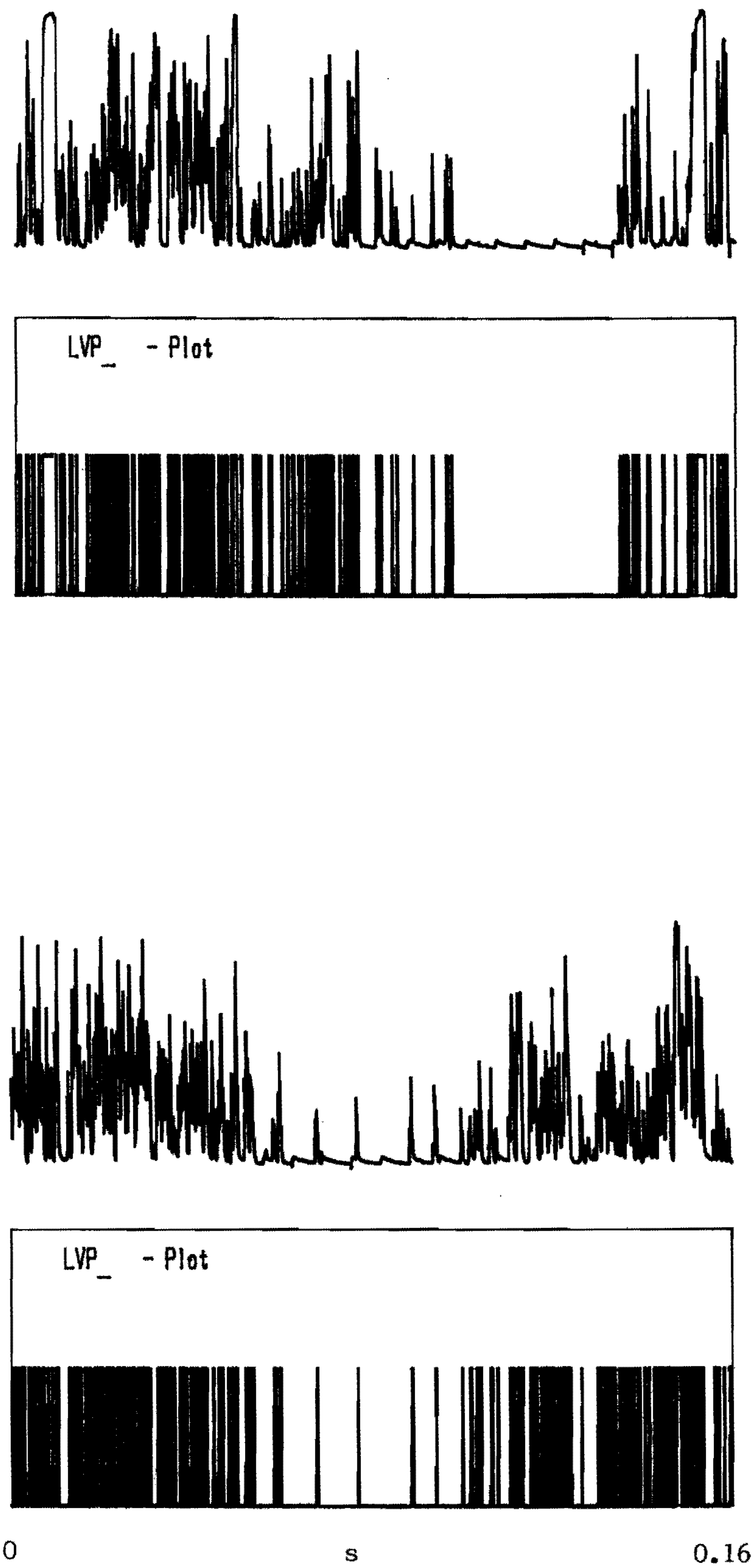

P = 40 bar

Q_{prehea} = 87.5 kW

Q_{testse} = 42 kW

Void fraction calculated from figure: 28 %

P = 40 bar

Q_{prehea} = 98 kW

Q_{testse} = 49 kW

Void fraction calculated from figure: 34 %

Figure 2.6

Recording and analysis of local void probe signals

of agglomoration of bubbles under the influence of hydrodynamical forces such as migration in axial and radial direction. Observation of this phenomenon is made possible by the long length of the testsection.
Intermittend flows at higher heating powers are often designated as "frothian" with a low degree of certainty (see the appendix), which reveals accelerations as well as oscillations in the mass flow rate, that also have been observed directly with the flow restrictions (section 2.4.3).
The comparisons with the Griffith and Wallis flow pattern map show that this is a rather course flow pattern delineation. Notice that their "slug" regime is the type of flow that is "intermittend" of "froth" in our terminolgy.

APPENDIX

GLOSSERY

BUBBLE 1	homogeneous bubble flow ; uniformly distributed (ellipsoïdal) bubbles
BUBBLE 2	heterogeneous bubble flow with a swirling bubble train and the higher velocities in the centre of the tube
BUBBLE 3	heterogeneous bubble flow , dispersed, with regions of highly concentrated bubbles in the centre of the tube. Occurs at higher flow rates.
DEV.LI.PLUG	transition regime between bubble 2 and little plug flow which easily can be obeserved and recognised both with the eye and the Flow Pattern Indicator
LITTLE PLUG	flow with short vapor plugs/pockets with axial length's of about 1 D (tube diameter). Upper limmit about 1½ D.
PLUG 1	vapor pockets with length's of about 4D ; upper limit 6D
PLUG 2	vapor pockets with length's of about 16D
SEMI CHURN	strongly pulsating flow with large slugs of vapor and with irregular liquid bridgings and much to-and-fro motion. The vapor slugs can hardly be recognised with the eye.
FROTH	weakly pulsating flow with alternate slugs of gas and liquid occurring only at higher flow rates. Many small bubbles seem to cover up the tube wall. There is not as much to-and-fro motion as in semi-churn flow. Near the wall the flow is essentially upward in both froth1 and froth2 with the higher velocities occurring in froth1
CHURN	heavily pulsating flow without distinct vapor pockets but with very much to-and-fro motion. Strong oscillatory behaviour.
BUBBLE 1A	is BUBBLE 1 with more certainty than BUBBLE 1B etc. etc.. In fact when BUBBLE 1B is measured it is better to repeat the measurement once again. The next result may be more conclusive ; this gradation turns out to be useful in transition regions between distinct flow patterns
MAXRANGE	maximum in measured top-top values of FPI-signals of all flow patterns
RANGE	maximum in top-top values of a signal for some interval of observation, divided by the MAXRANGE
AR	range of the centre flag in %
BR	range of the flag near the wall in %
AT	number of tops per 5 sec of the centre flag
AP	number of pikes per 5 sec of the centre flag

LITERATURE AND REFERENCES

Bennett, A.W.; Hewitt, G.F.; Kearsy, H.A.;Keeys, R.K.F. and Lacey, P.M.C.
Flow visualisation studies of boiling at high pressure.
AERE-R4874, Harwell, 1965.

Geld, C.W.M. van der
Flow regime recognition at elevated pressures
European Two-phase Flow Group Meeting, Rome, 1984.
Report nr. WOP-WET 84.009, Eindhoven University of Technology.

Govier, G.W.; Radford, B.A. and Dunn, J.S.C.
Can. J. Chem. Eng., 35, page 58, 1957.

Griffith, P. and Wallis, G.B.
Trans. ASME, C83, page 307, 1961.

Tippets, F.E.
Critical heat fluxes and flow patterns in high-pressure boiling water flows.
J. of Heat Transfer, Trans. of the ASME, page 12, 1964.

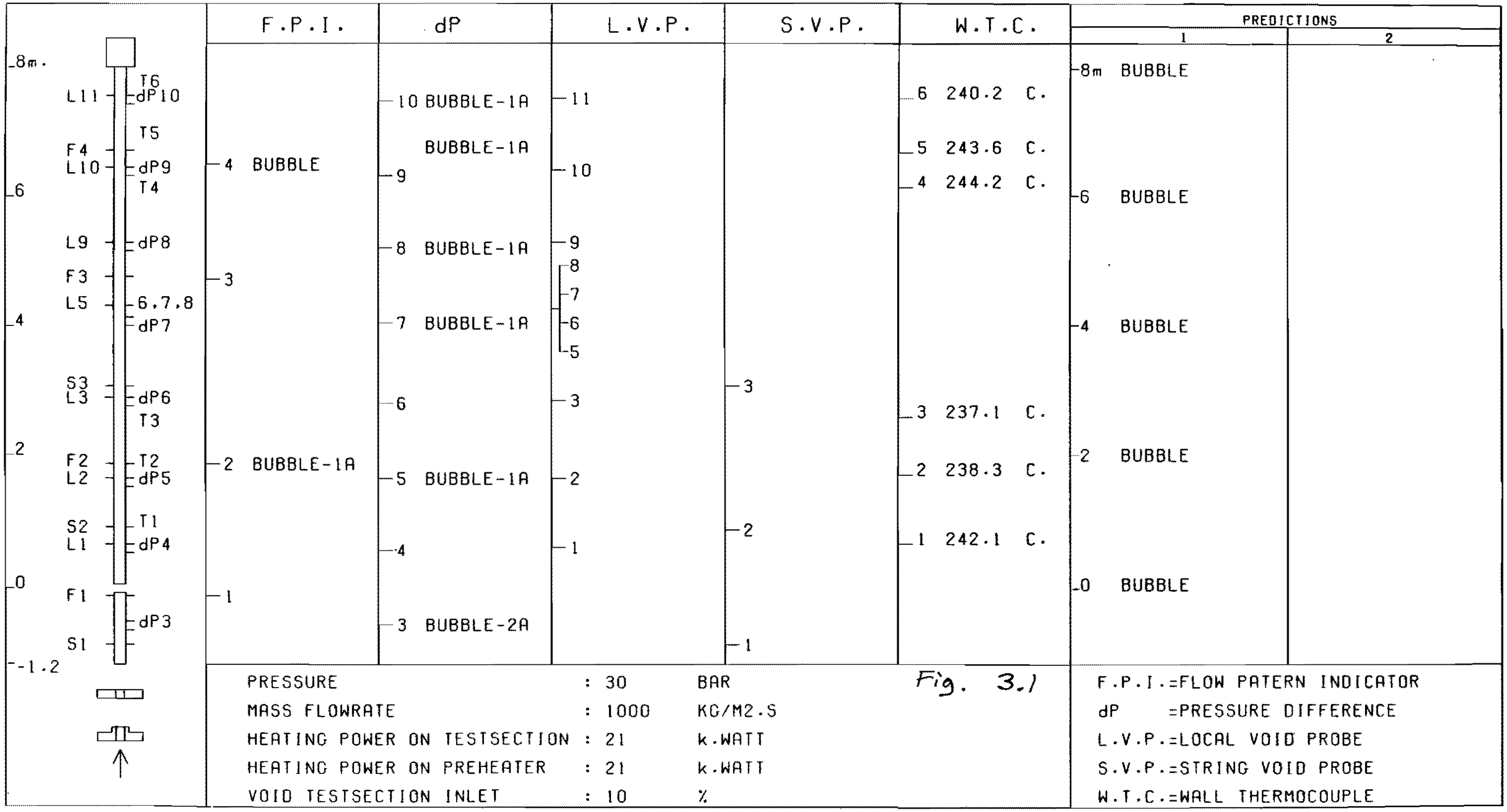

Fig. 3.1

PRESSURE	:	30	BAR
MASS FLOWRATE	:	1000	KG/M2.S
HEATING POWER ON TESTSECTION	:	21	k.WATT
HEATING POWER ON PREHEATER	:	21	k.WATT
VOID TESTSECTION INLET	:	10	%

F.P.I.=FLOW PATERN INDICATOR
dP =PRESSURE DIFFERENCE
L.V.P.=LOCAL VOID PROBE
S.V.P.=STRING VOID PROBE
W.T.C.=WALL THERMOCOUPLE

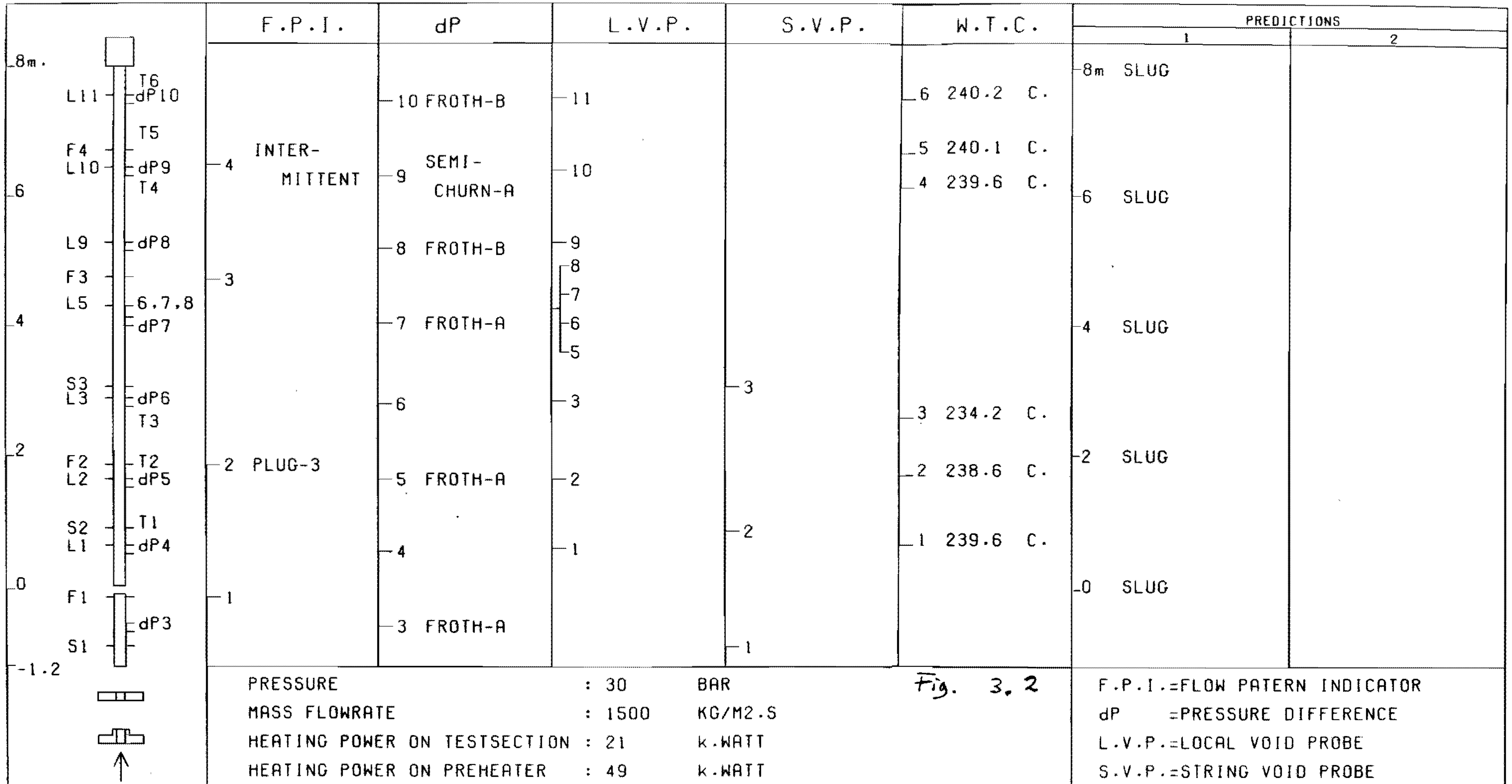

PRESSURE	:	30	BAR
MASS FLOWRATE	:	1500	KG/M2.S
HEATING POWER ON TESTSECTION	:	21	k.WATT
HEATING POWER ON PREHEATER	:	49	k.WATT
VOID TESTSECTION INLET	:	22	%

Fig. 3.2

F.P.I.=FLOW PATERN INDICATOR
dP =PRESSURE DIFFERENCE
L.V.P.=LOCAL VOID PROBE
S.V.P.=STRING VOID PROBE
W.T.C.=WALL THERMOCOUPLE

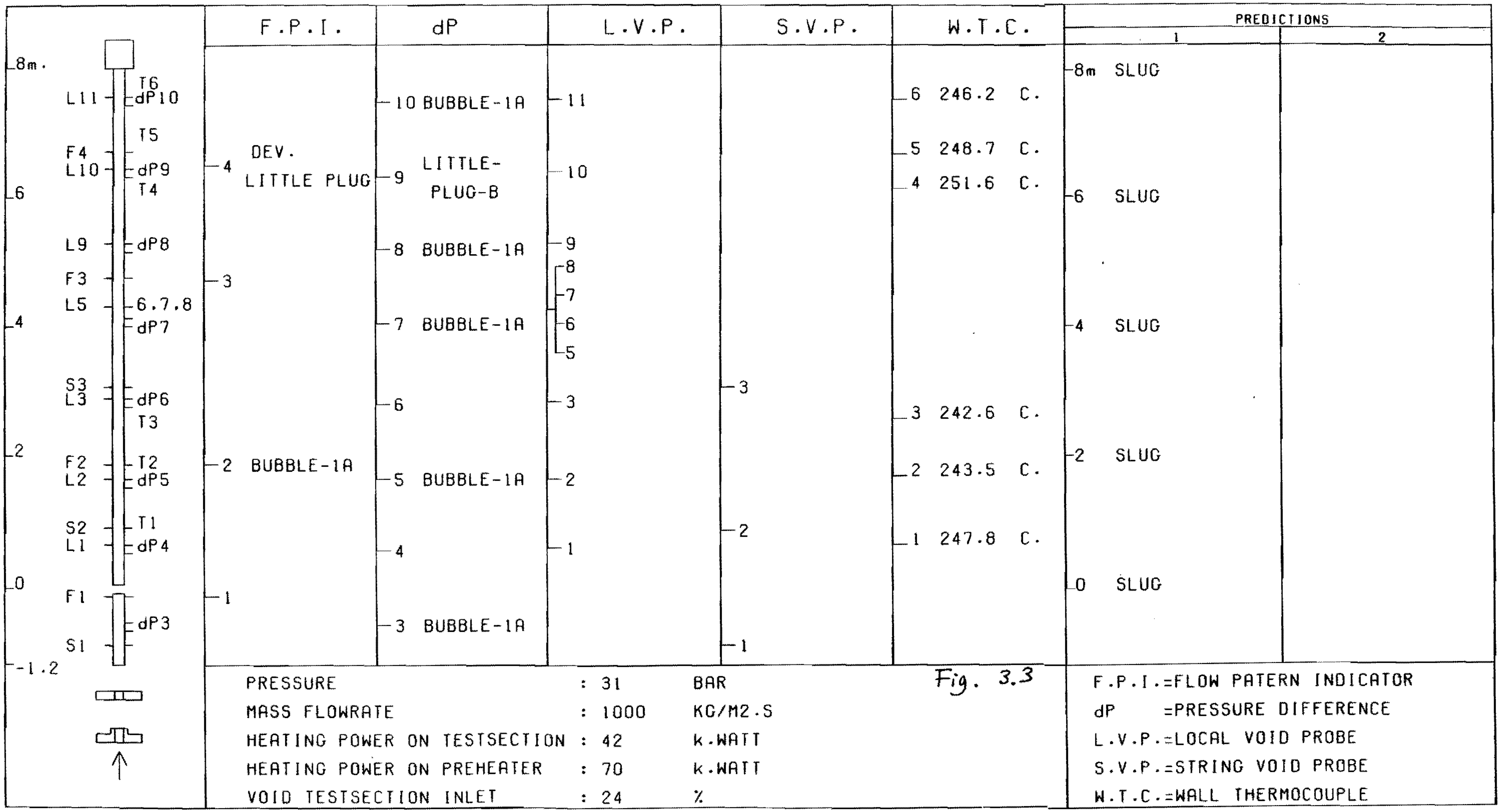
F.P.I.
dP
L.V.P.
S.V.P.
W.T.C.
PREDICTIONS
1
2
8m.
6
4
2
0
-1.2
L11
F4
L10
L9
F3
L5
S3
L3
F2
L2
S2
L1
F1
S1
T6
dP10
T5
dP9
T4
dP8
6.7.8
dP7
dP6
T3
T2
dP5
T1
dP4
dP3
4 DEV. LITTLE PLUG
3
2 BUBBLE-1A
1
10 BUBBLE-1A
9 LITTLE-PLUG-B
8 BUBBLE-1A
7 BUBBLE-1A
6
5 BUBBLE-1A
4
3 BUBBLE-1A
11
10
9
8
7
6
5
3
2
1
3
2
1
6 246.2 C.
5 248.7 C.
4 251.6 C.
3 242.6 C.
2 243.5 C.
1 247.8 C.
8m SLUG
6 SLUG
4 SLUG
2 SLUG
0 SLUG
PRESSURE : 31 BAR
MASS FLOWRATE : 1000 KG/M2.S
HEATING POWER ON TESTSECTION : 42 k.WATT
HEATING POWER ON PREHEATER : 70 k.WATT
VOID TESTSECTION INLET : 24 %
F.P.I.=FLOW PATERN INDICATOR
dP =PRESSURE DIFFERENCE
L.V.P.=LOCAL VOID PROBE
S.V.P.=STRING VOID PROBE
W.T.C.=WALL THERMOCOUPLE

Fig. 3.3

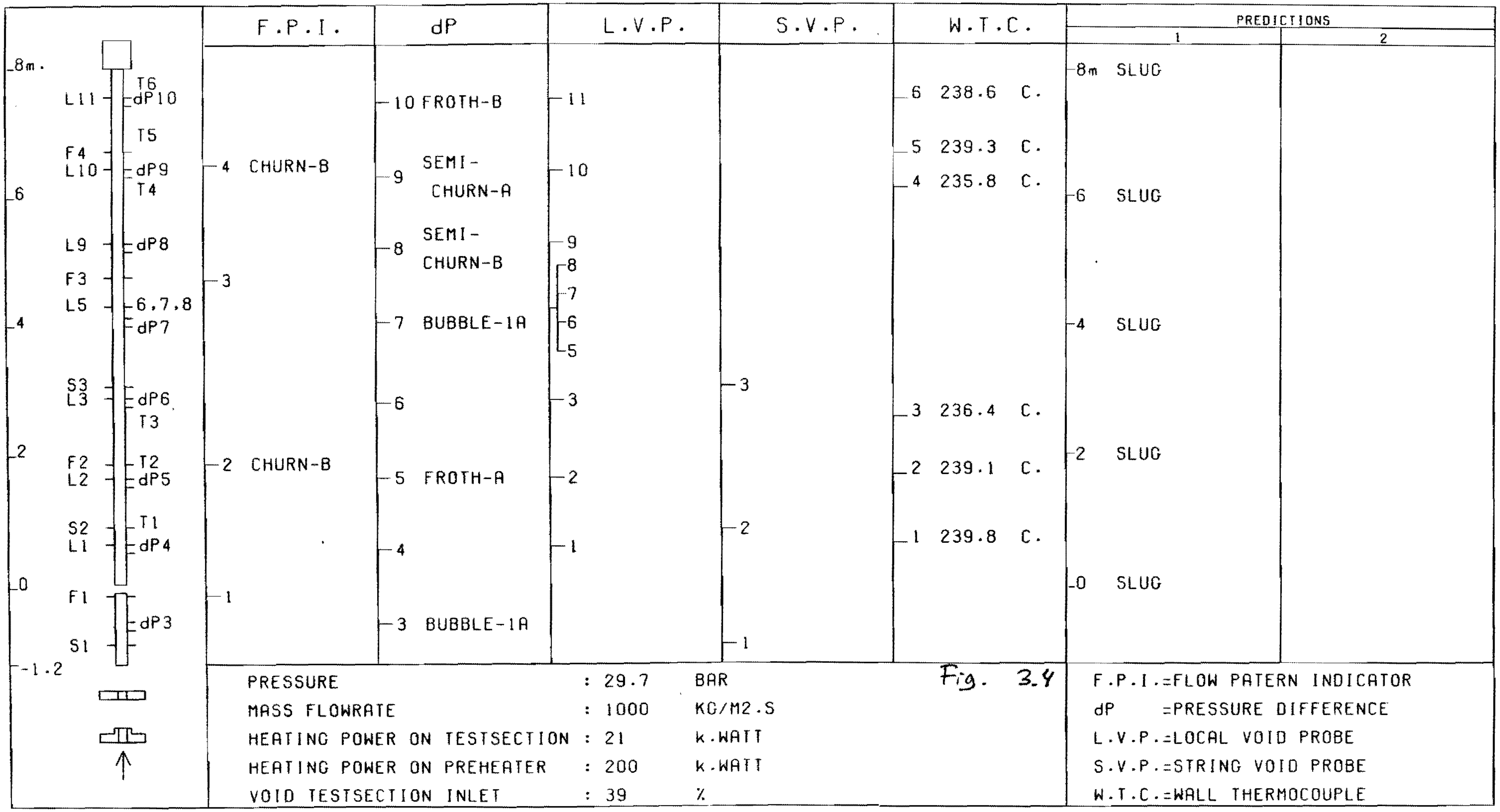

F.P.I.
dP
L.V.P.
S.V.P.
W.T.C.
PREDICTIONS
1
2
8m.
6
4
2
0
-1.2
L11
T6
dP10
T5
F4
L10
dP9
T4
L9
dP8
F3
L5
6,7,8
dP7
S3
L3
dP6
T3
F2
L2
T2
dP5
S2
L1
T1
dP4
F1
dP3
S1
4 CHURN-B
3
2 CHURN-B
1
10 FROTH-B
9 SEMI-CHURN-A
8 SEMI-CHURN-B
7 BUBBLE-1A
6
5 FROTH-A
4
3 BUBBLE-1A
11
10
9
8
7
6
5
3
2
1
3
2
1
6 238.6 C.
5 239.3 C.
4 235.8 C.
3 236.4 C.
2 239.1 C.
1 239.8 C.
8m SLUG
6 SLUG
4 SLUG
2 SLUG
0 SLUG
PRESSURE : 29.7 BAR
MASS FLOWRATE : 1000 KG/M2.S
HEATING POWER ON TESTSECTION : 21 k.WATT
HEATING POWER ON PREHEATER : 200 k.WATT
VOID TESTSECTION INLET : 39 %
F.P.I.=FLOW PATERN INDICATOR
dP =PRESSURE DIFFERENCE
L.V.P.=LOCAL VOID PROBE
S.V.P.=STRING VOID PROBE
W.T.C.=WALL THERMOCOUPLE

Fig. 3.4

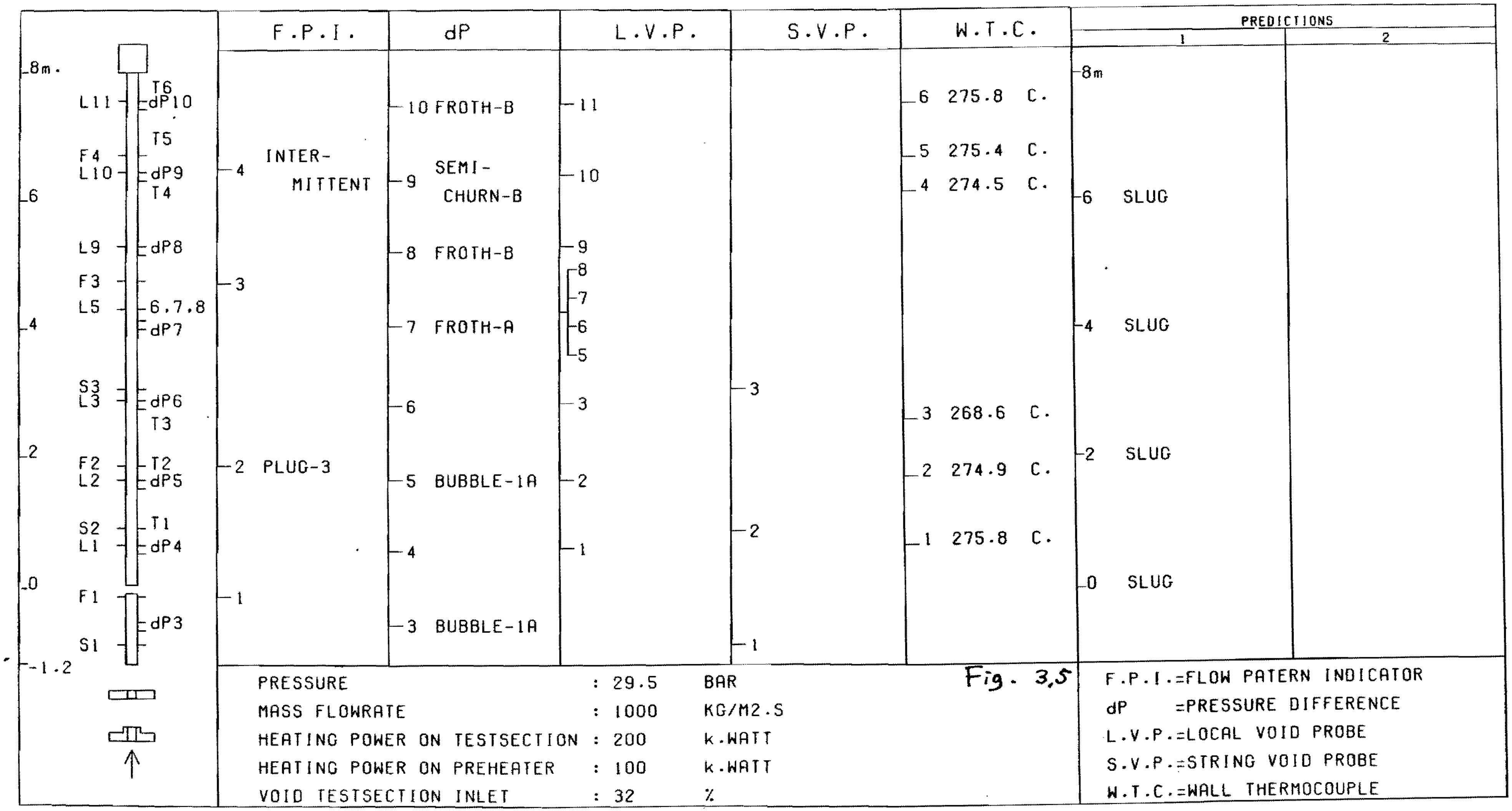
F.P.I.
dP
L.V.P.
S.V.P.
W.T.C.
PREDICTIONS
1
2
8m.
6
4
2
0
-1.2
L11
T6
dP10
T5
F4
L10
dP9
T4
L9
dP8
F3
L5
6,7,8
dP7
S3
L3
dP6
T3
F2
L2
T2
dP5
S2
L1
T1
dP4
F1
dP3
S1
INTER-
MITTENT
PLUG-3
10 FROTH-B
9 SEMI-
CHURN-B
8 FROTH-B
7 FROTH-A
5 BUBBLE-1A
3 BUBBLE-1A
6 275.8 C.
5 275.4 C.
4 274.5 C.
3 268.6 C.
2 274.9 C.
1 275.8 C.
8m
6 SLUG
4 SLUG
2 SLUG
0 SLUG
PRESSURE : 29.5 BAR
MASS FLOWRATE : 1000 KG/M2.S
HEATING POWER ON TESTSECTION : 200 k.WATT
HEATING POWER ON PREHEATER : 100 k.WATT
VOID TESTSECTION INLET : 32 %
F.P.I.=FLOW PATERN INDICATOR
dP =PRESSURE DIFFERENCE
L.V.P.=LOCAL VOID PROBE
S.V.P.=STRING VOID PROBE
W.T.C.=WALL THERMOCOUPLE

Fig. 3,5

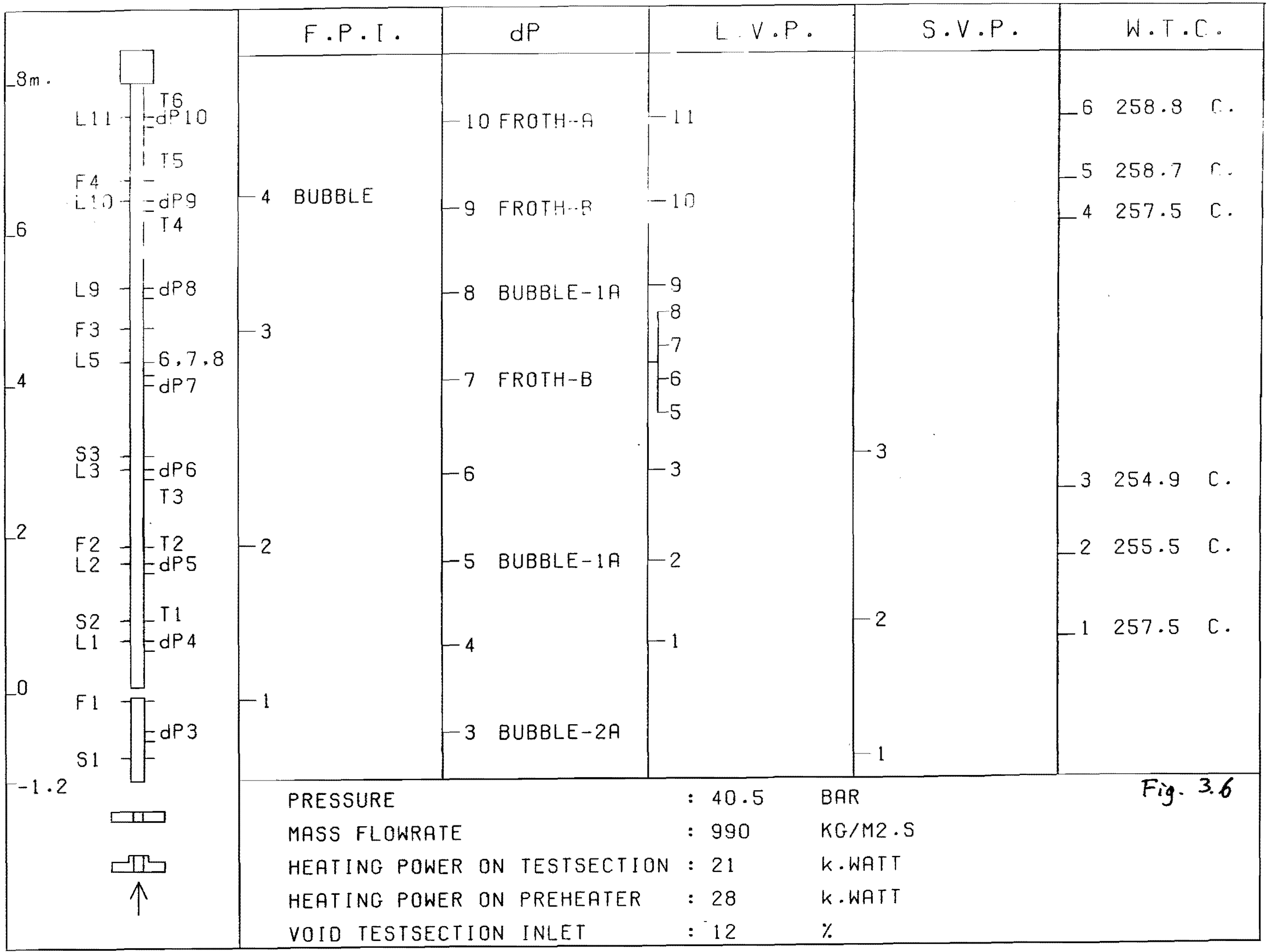

Fig. 3.6

PRESSURE	:	40.5	BAR
MASS FLOWRATE	:	990	KG/M2.S
HEATING POWER ON TESTSECTION	:	21	k.WATT
HEATING POWER ON PREHEATER	:	28	k.WATT
VOID TESTSECTION INLET	:	12	%

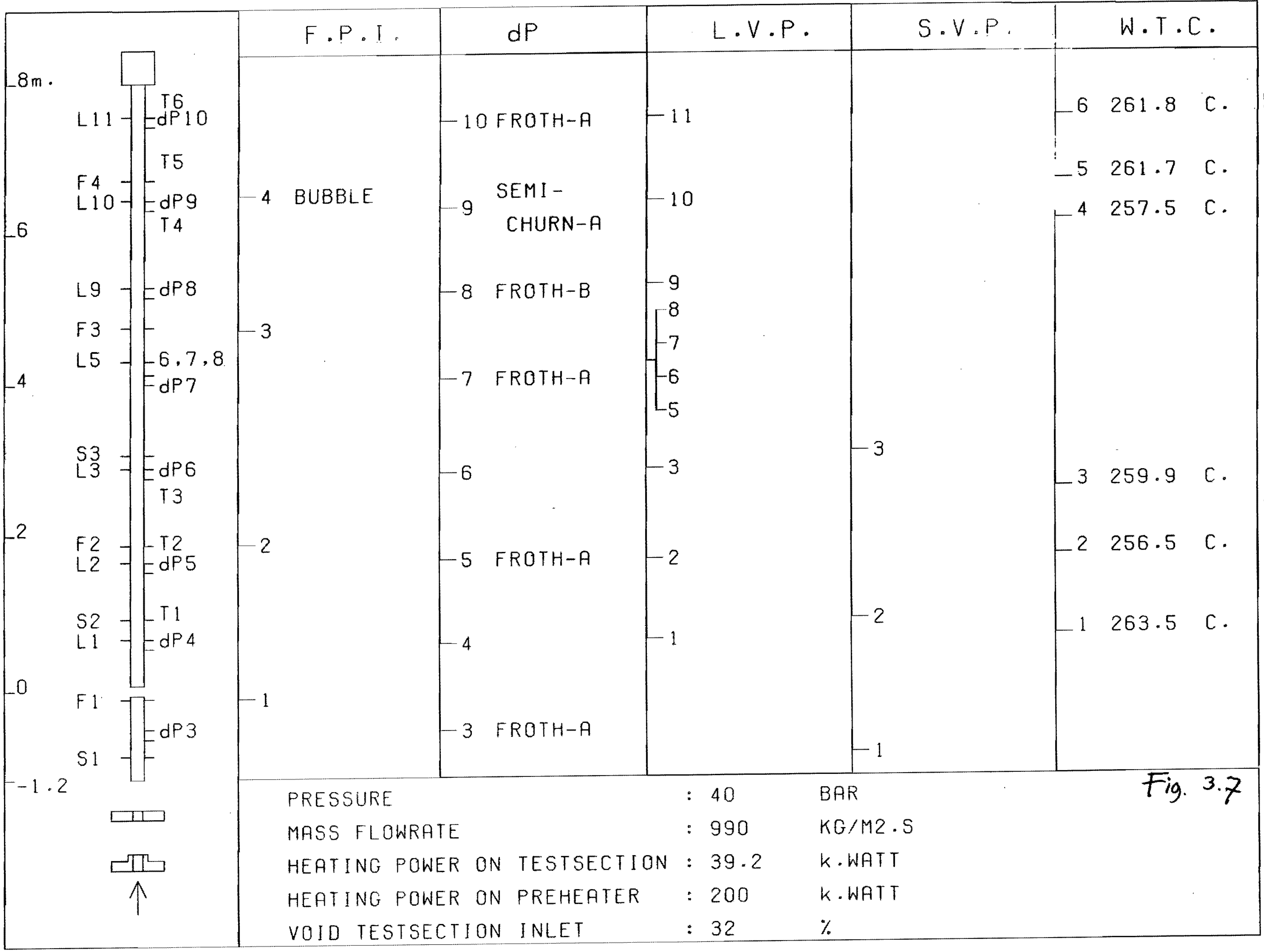
8m.
6
4
2
0
-1.2
T6
L11
dP10
T5
F4
L10
dP9
T4
L9
dP8
F3
L5
6,7,8
dP7
S3
L3
dP6
T3
F2
T2
L2
dP5
S2
T1
L1
dP4
F1
dP3
S1
F.P.I.
4 BUBBLE
3
2
1
dP
10 FROTH-A
9 SEMI-CHURN-A
8 FROTH-B
7 FROTH-A
6
5 FROTH-A
4
3 FROTH-A
L.V.P.
11
10
9
8
7
6
5
3
2
1
S.V.P.
3
2
1
W.T.C.
6 261.8 C.
5 261.7 C.
4 257.5 C.
3 259.9 C.
2 256.5 C.
1 263.5 C.
PRESSURE : 40 BAR
MASS FLOWRATE : 990 KG/M2.S
HEATING POWER ON TESTSECTION : 39.2 k.WATT
HEATING POWER ON PREHEATER : 200 k.WATT
VOID TESTSECTION INLET : 32 %

Fig. 3.7

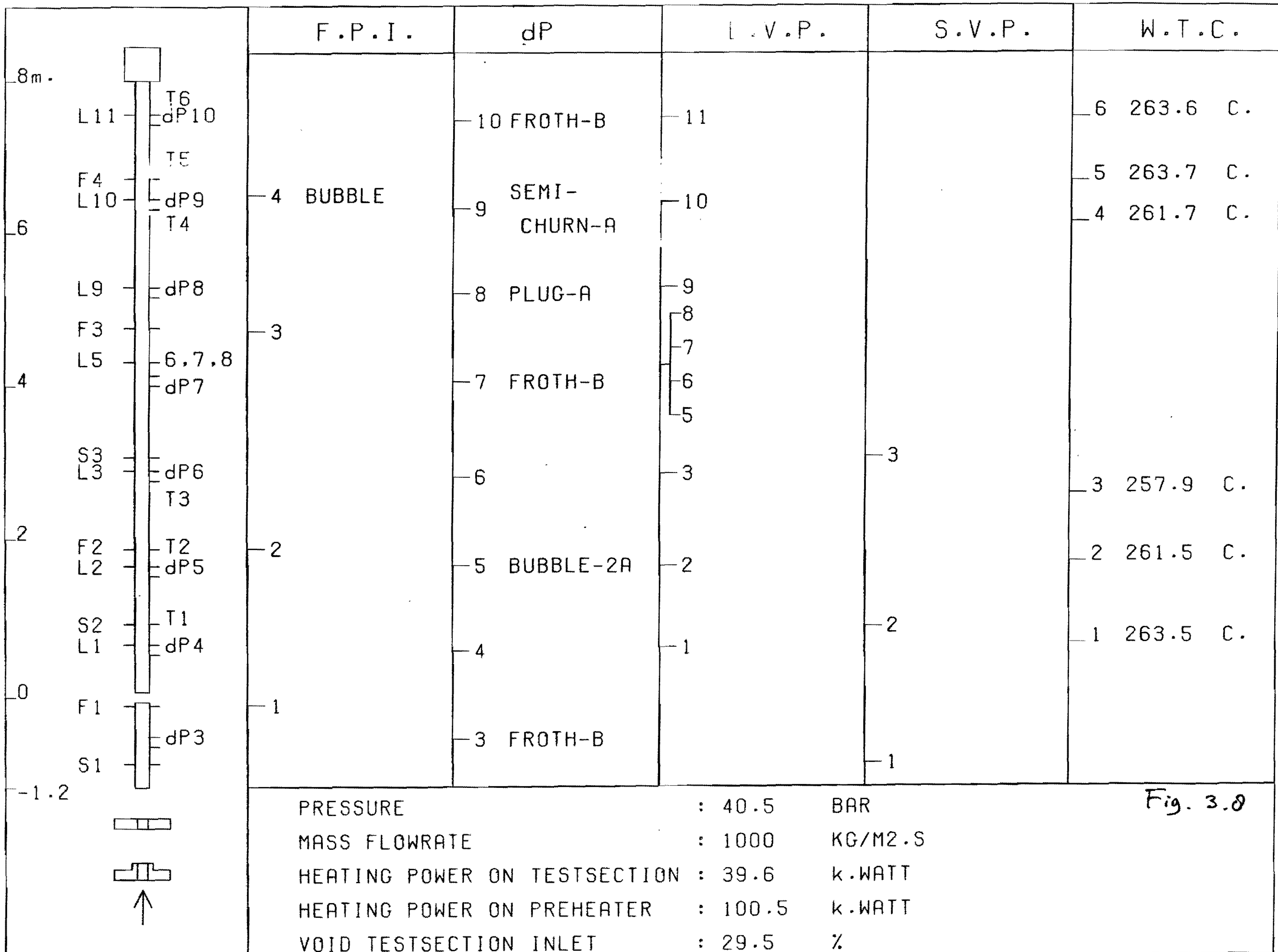

PRESSURE	: 40.5	BAR
MASS FLOWRATE	: 1000	KG/M2.S
HEATING POWER ON TESTSECTION	: 39.6	k.WATT
HEATING POWER ON PREHEATER	: 100.5	k.WATT
VOID TESTSECTION INLET	: 29.5	%

Fig. 3.8

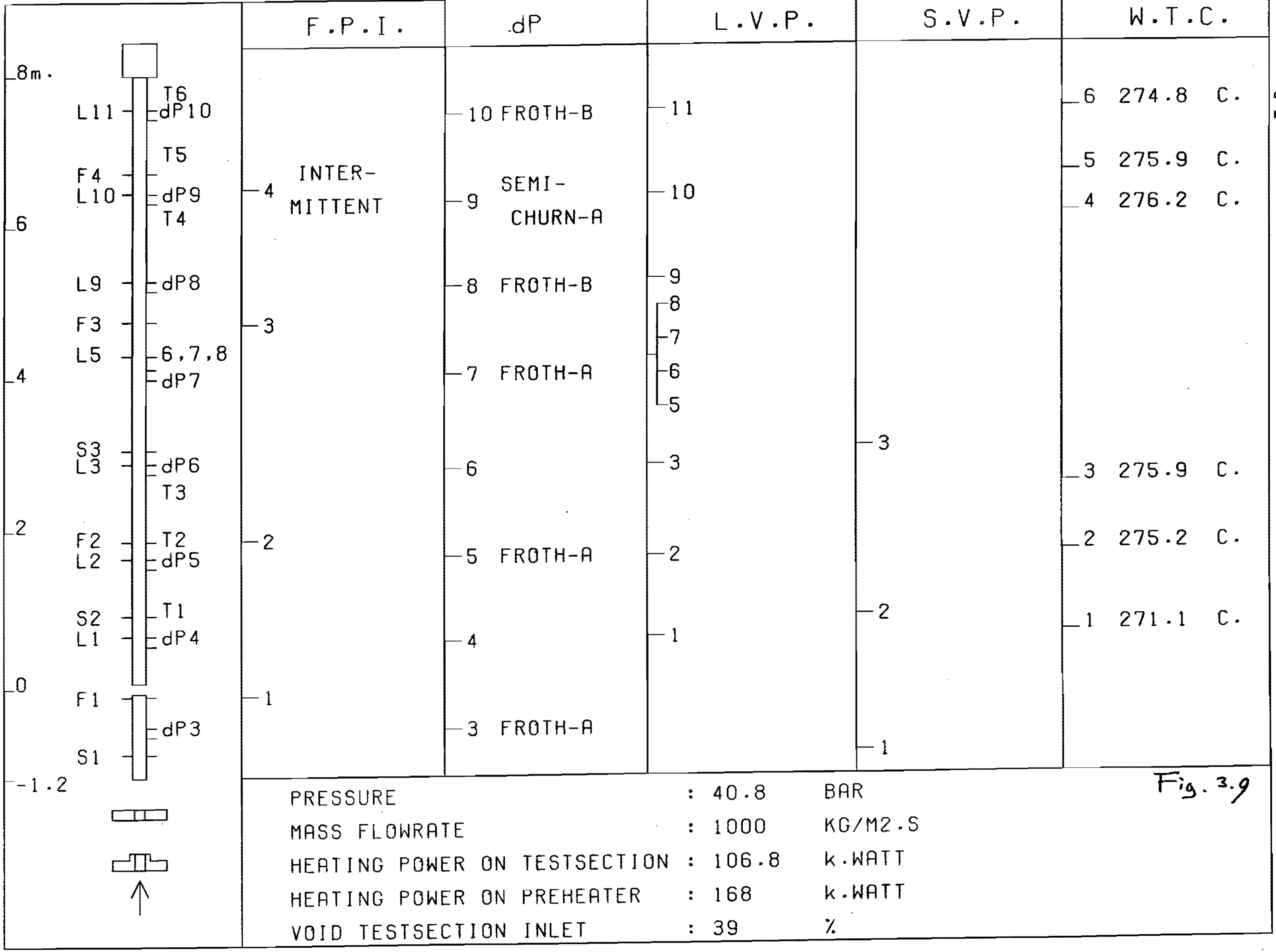
F.P.I.
dP
L.V.P.
S.V.P.
W.T.C.
8m.
6
4
2
0
-1.2
L11
T6
dP10
T5
F4
L10
dP9
T4
L9
dP8
F3
L5
6,7,8
dP7
S3
L3
dP6
T3
F2
T2
L2
dP5
S2
T1
L1
dP4
F1
dP3
S1
4 INTER-MITTENT
3
2
1
10 FROTH-B
9 SEMI-CHURN-A
8 FROTH-B
7 FROTH-A
6
5 FROTH-A
4
3 FROTH-A
11
10
9
8
7
6
5
3
2
1
3
2
1
6 274.8 C.
5 275.9 C.
4 276.2 C.
3 275.9 C.
2 275.2 C.
1 271.1 C.
PRESSURE : 40.8 BAR
MASS FLOWRATE : 1000 KG/M2.S
HEATING POWER ON TESTSECTION : 106.8 k.WATT
HEATING POWER ON PREHEATER : 168 k.WATT
VOID TESTSECTION INLET : 39 %

Fig. 3.9

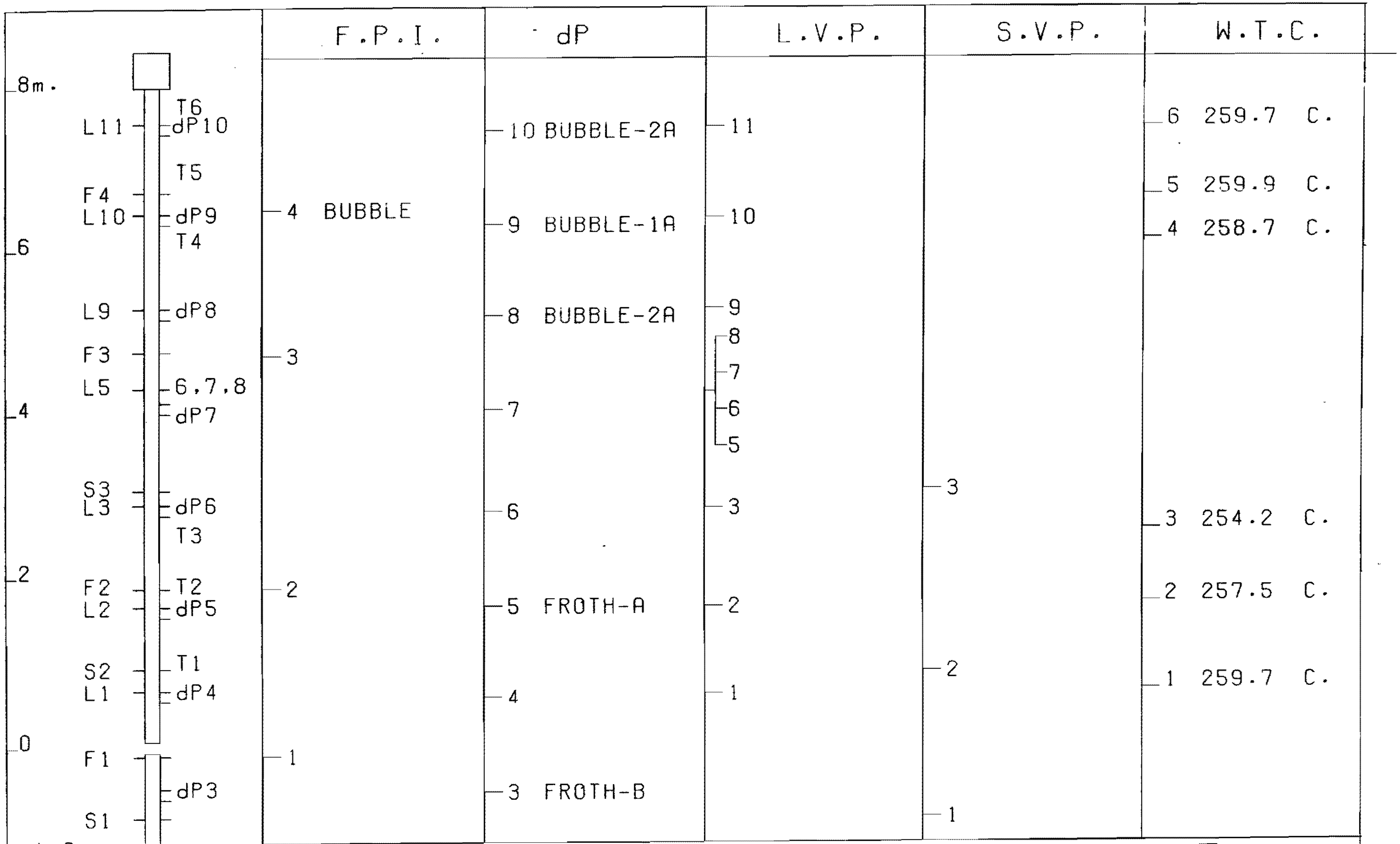

Fig. 3.10

PRESSURE	:	40	BAR
MASS FLOWRATE	:	830	KG/M2.S
HEATING POWER ON TESTSECTION	:	21	k.WATT
HEATING POWER ON PREHEATER	:	7	k.WATT

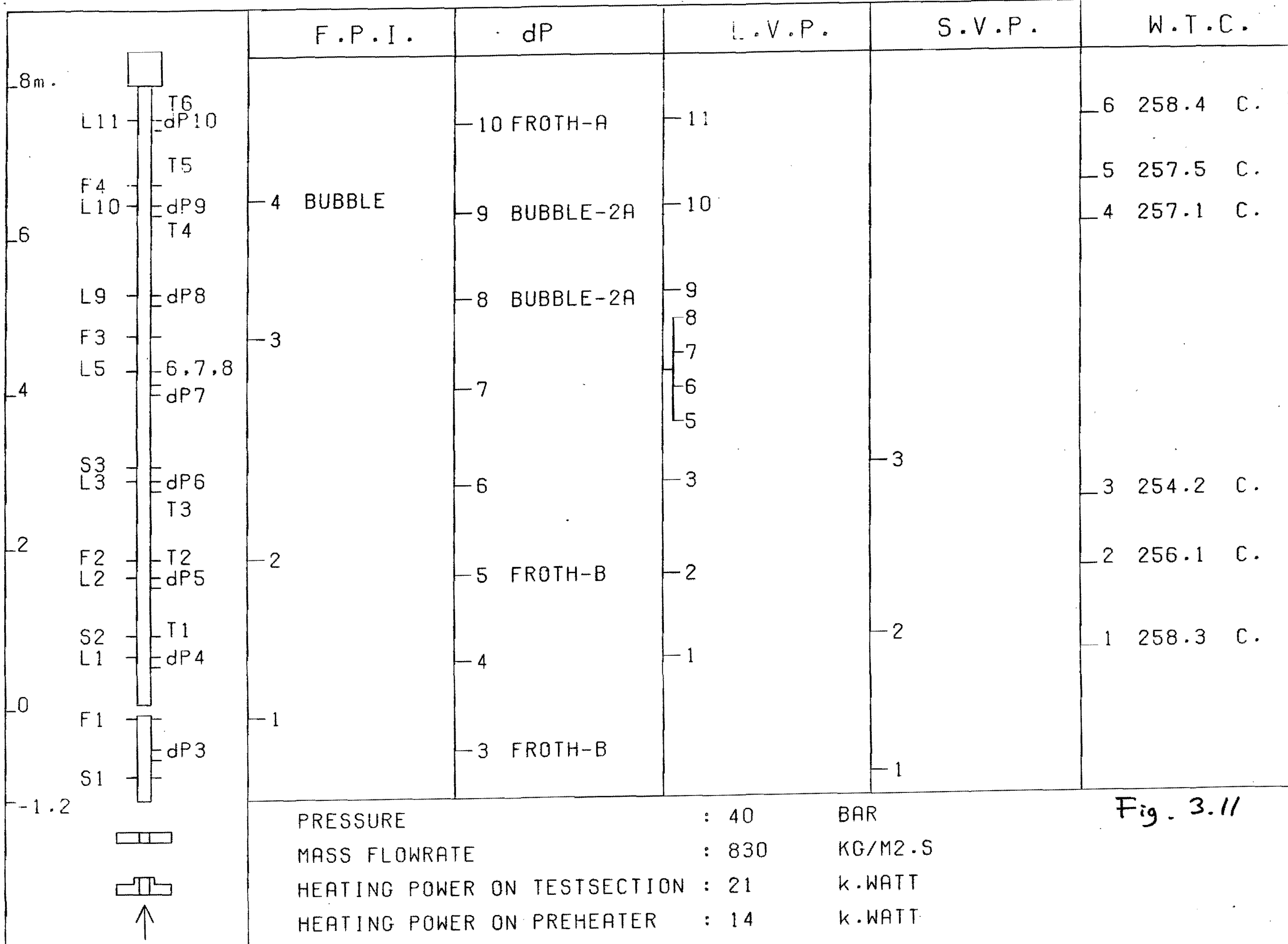

PRESSURE	: 40	BAR
MASS FLOWRATE	: 830	KG/M2.S
HEATING POWER ON TESTSECTION	: 21	k.WATT
HEATING POWER ON PREHEATER	: 14	k.WATT
VOID TESTSECTION INLET	:	%

Fig. 3.11

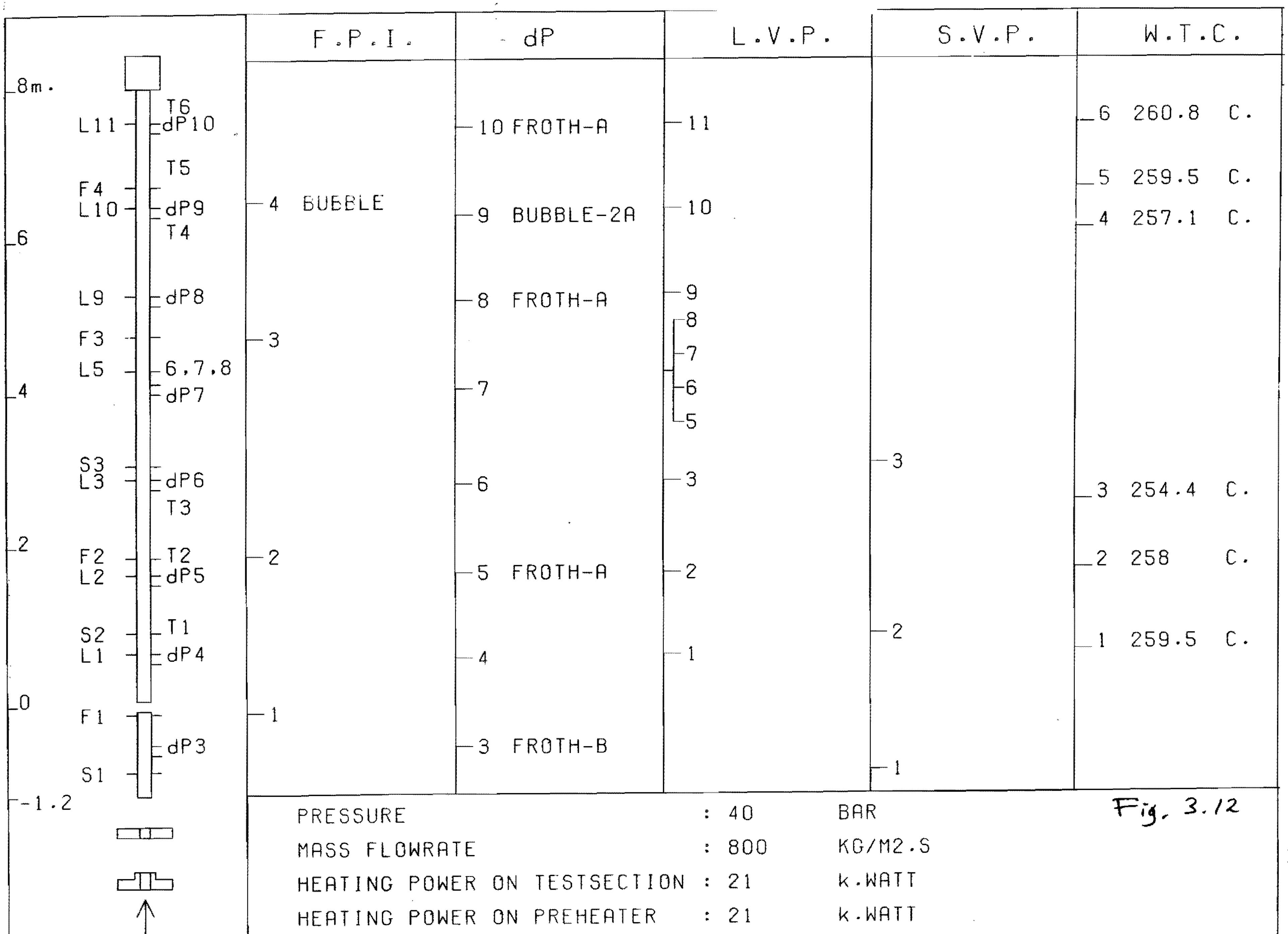

PRESSURE	:	40	BAR
MASS FLOWRATE	:	800	KG/M2.S
HEATING POWER ON TESTSECTION	:	21	k.WATT
HEATING POWER ON PREHEATER	:	21	k.WATT
VOID TESTSECTION INLET	:		%

Fig. 3.12

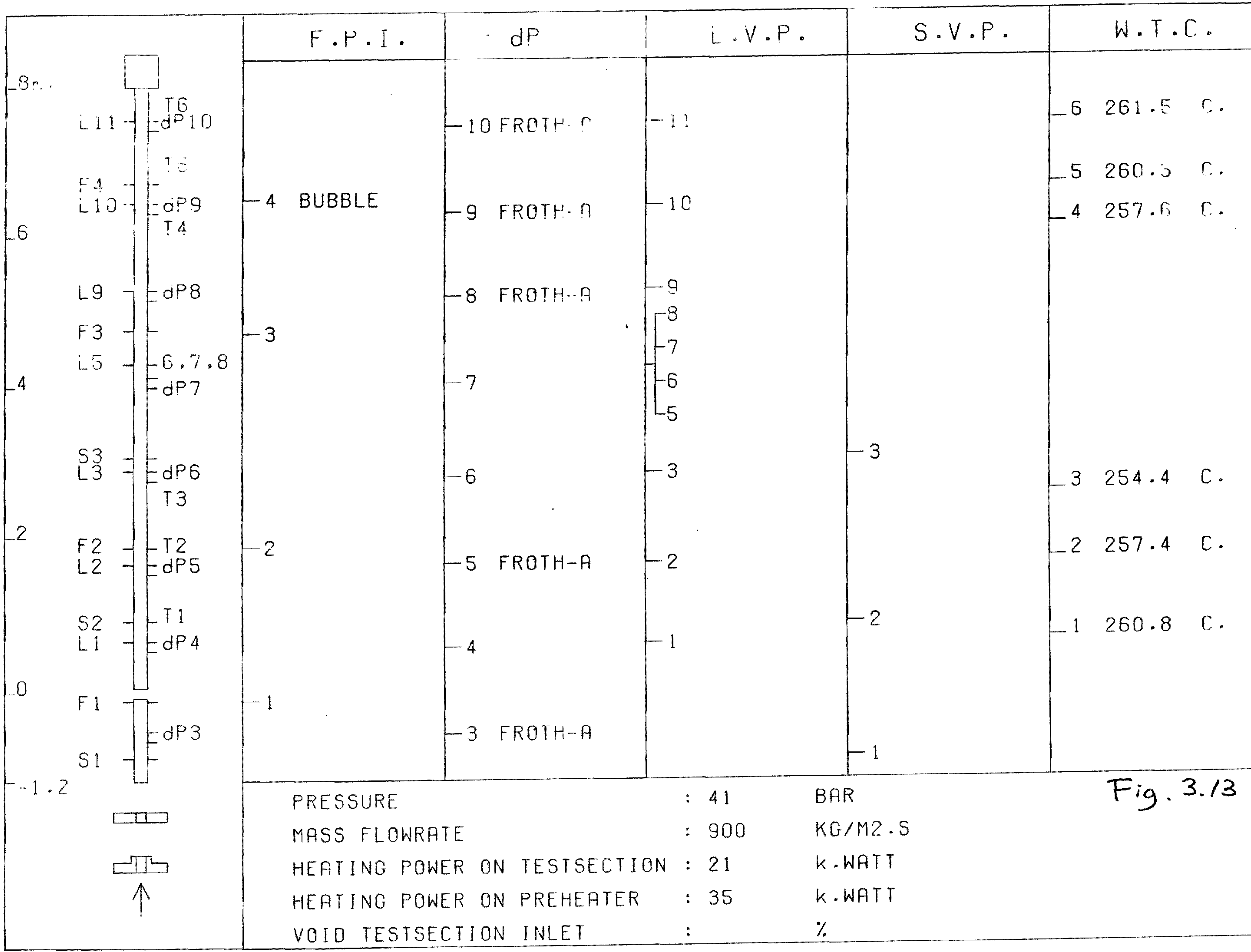
F.P.I.
dP
L.V.P.
S.V.P.
W.T.C.
8m
6
4
2
0
-1.2
L11
F4
L10
L9
F3
L5
S3
L3
F2
L2
S2
L1
F1
S1
T6
dP10
T5
dP9
T4
dP8
6,7,8
dP7
dP6
T3
T2
dP5
T1
dP4
dP3
4 BUBBLE
3
2
1
10 FROTH-A
9 FROTH-A
8 FROTH-A
7
6
5 FROTH-A
4
3 FROTH-A
11
10
9
8
7
6
5
3
2
1
3
2
1
6 261.5 C.
5 260.5 C.
4 257.6 C.
3 254.4 C.
2 257.4 C.
1 260.8 C.
PRESSURE : 41 BAR
MASS FLOWRATE : 900 KG/M2.S
HEATING POWER ON TESTSECTION : 21 k.WATT
HEATING POWER ON PREHEATER : 35 k.WATT
VOID TESTSECTION INLET : %

Fig. 3.13

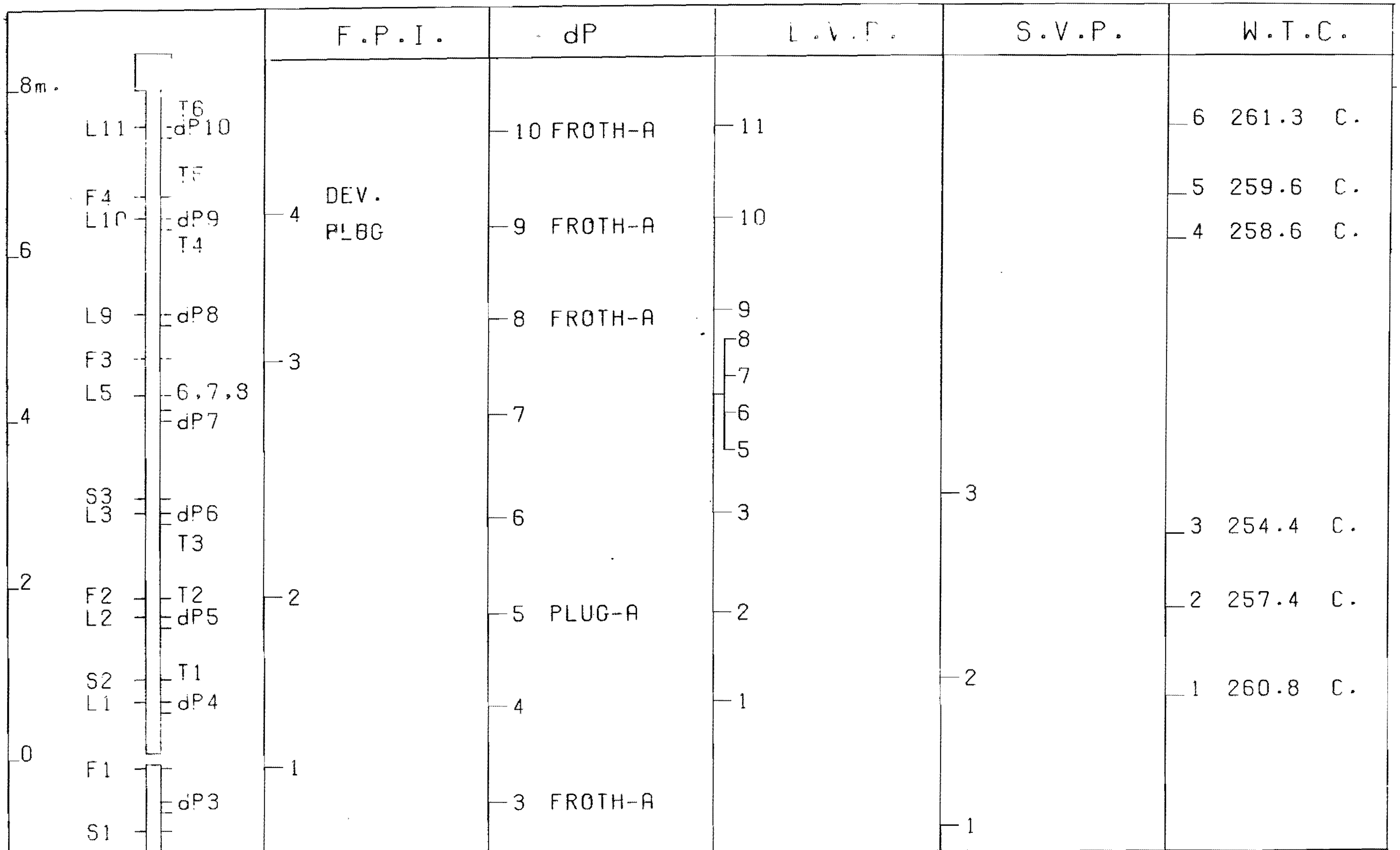

PRESSURE : 41 BAR

MASS FLOWRATE : 960 KG/M2.S

HEATING POWER ON TESTSECTION : 21 k.WATT

HEATING POWER ON PREHEATER : 56 k.WATT

Fig. 3.14

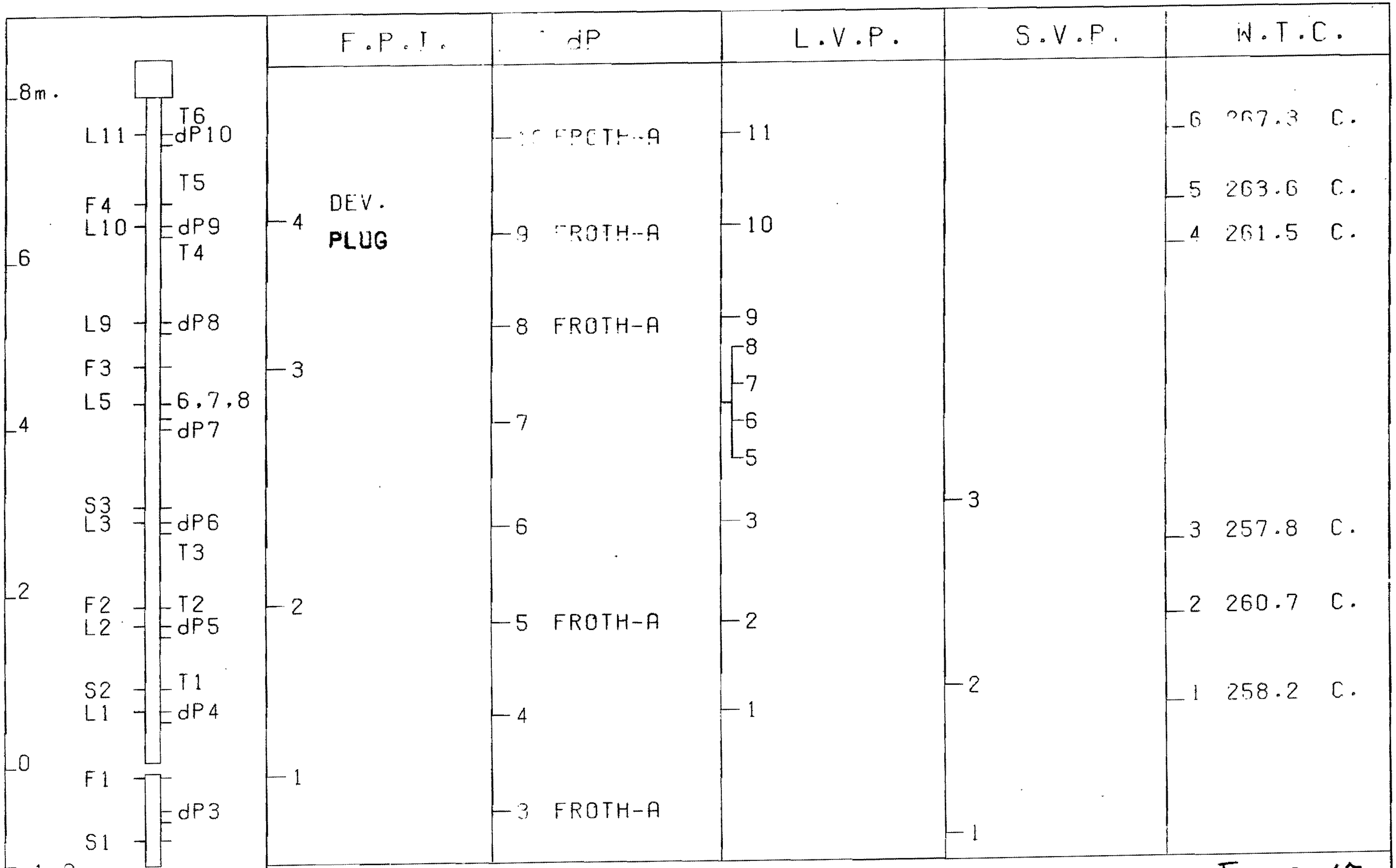

PRESSURE	:	41	BAR
MASS FLOWRATE	:	960	KG/M2.S
HEATING POWER ON TESTSECTION	:	35	k.WATT
HEATING POWER ON PREHEATER	:	77	k.WATT
VOID TESTSECTION INLET	:		%

Fig. 3.15

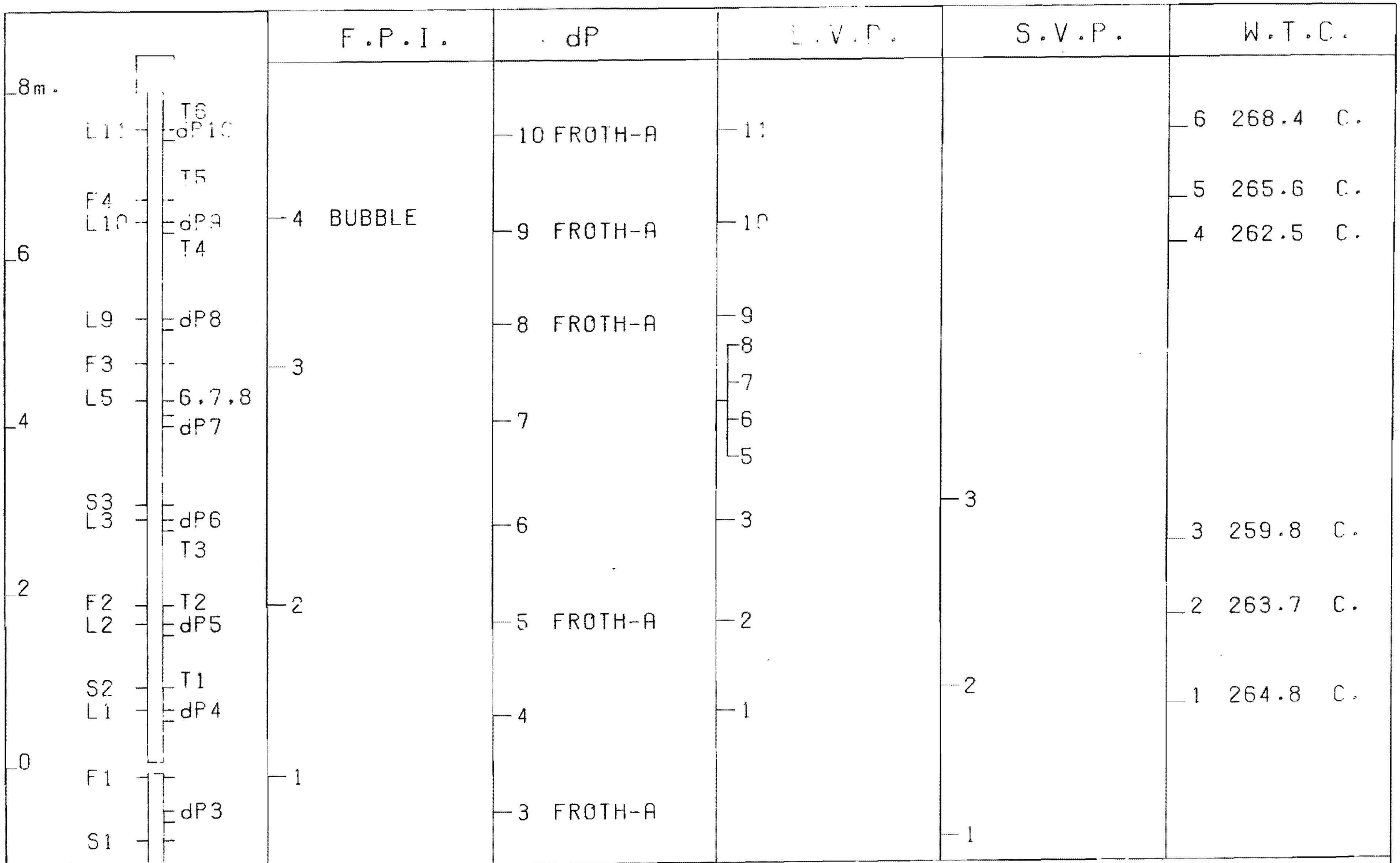

Fig. 3.16

PRESSURE	: 40	BAR
MASS FLOWRATE	: 960	KG/M2.S
HEATING POWER ON TESTSECTION	: 49	k.WATT
HEATING POWER ON PREHEATER	: 98	k.WATT
VOID TESTSECTION INLET	:	%

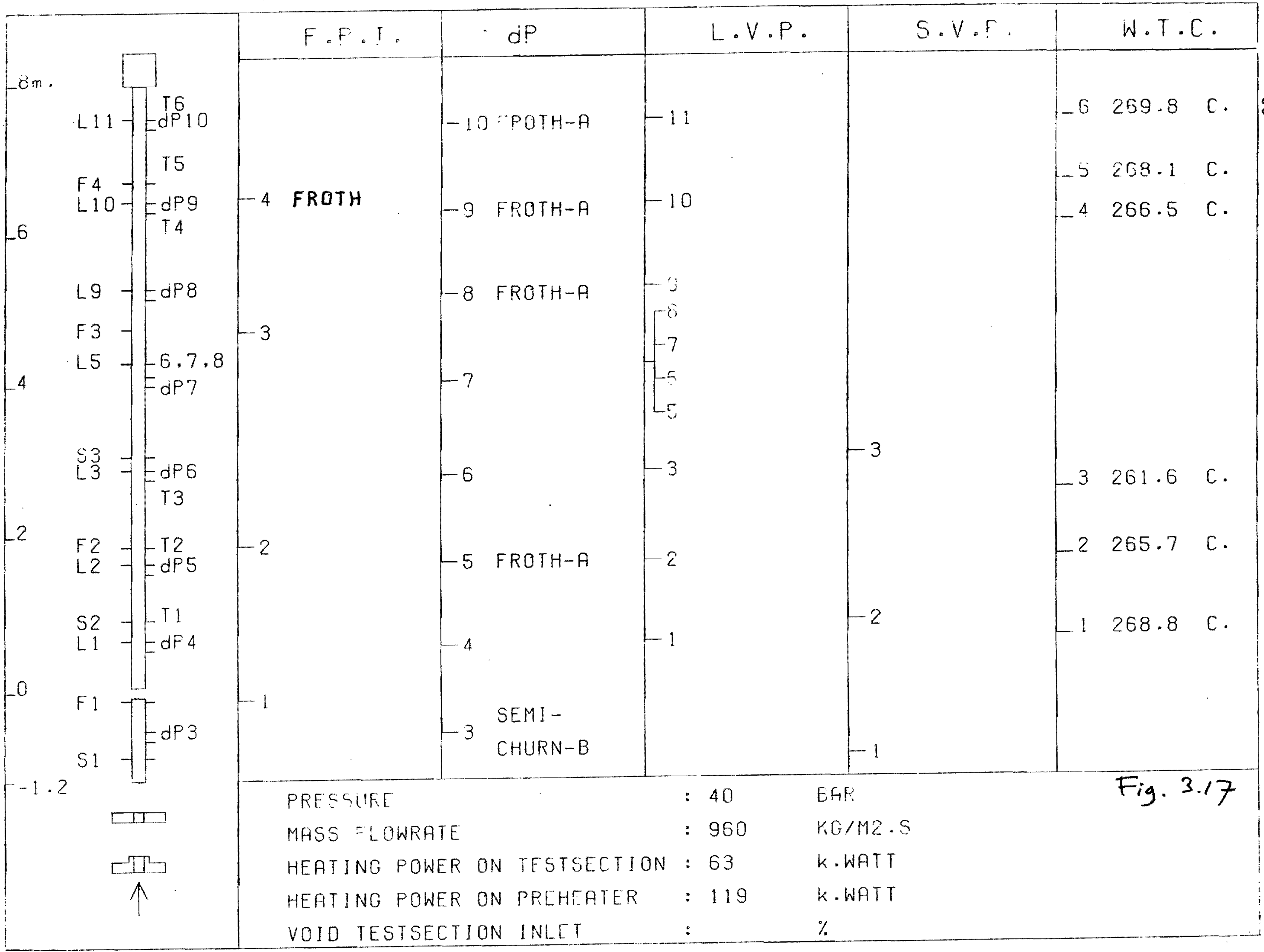
F.P.I.
dP
L.V.P.
S.V.F.
W.T.C.
8m.
6
4
2
0
-1.2
L11
T6
dP10
T5
F4
L10
dP9
T4
L9
dP8
F3
L5
6,7,8
dP7
S3
L3
dP6
T3
F2
L2
T2
dP5
S2
L1
T1
dP4
F1
dP3
S1
4 FROTH
3
2
1
10 FROTH-A
9 FROTH-A
8 FROTH-A
7
6
5 FROTH-A
4
3 SEMI-CHURN-B
11
10
9
8
7
6
5
3
2
1
3
2
1
6 269.8 C.
5 268.1 C.
4 266.5 C.
3 261.6 C.
2 265.7 C.
1 268.8 C.
PRESSURE : 40 BAR
MASS FLOWRATE : 960 KG/M2.S
HEATING POWER ON TESTSECTION : 63 k.WATT
HEATING POWER ON PREHEATER : 119 k.WATT
VOID TESTSECTION INLET : %

Fig. 3.17

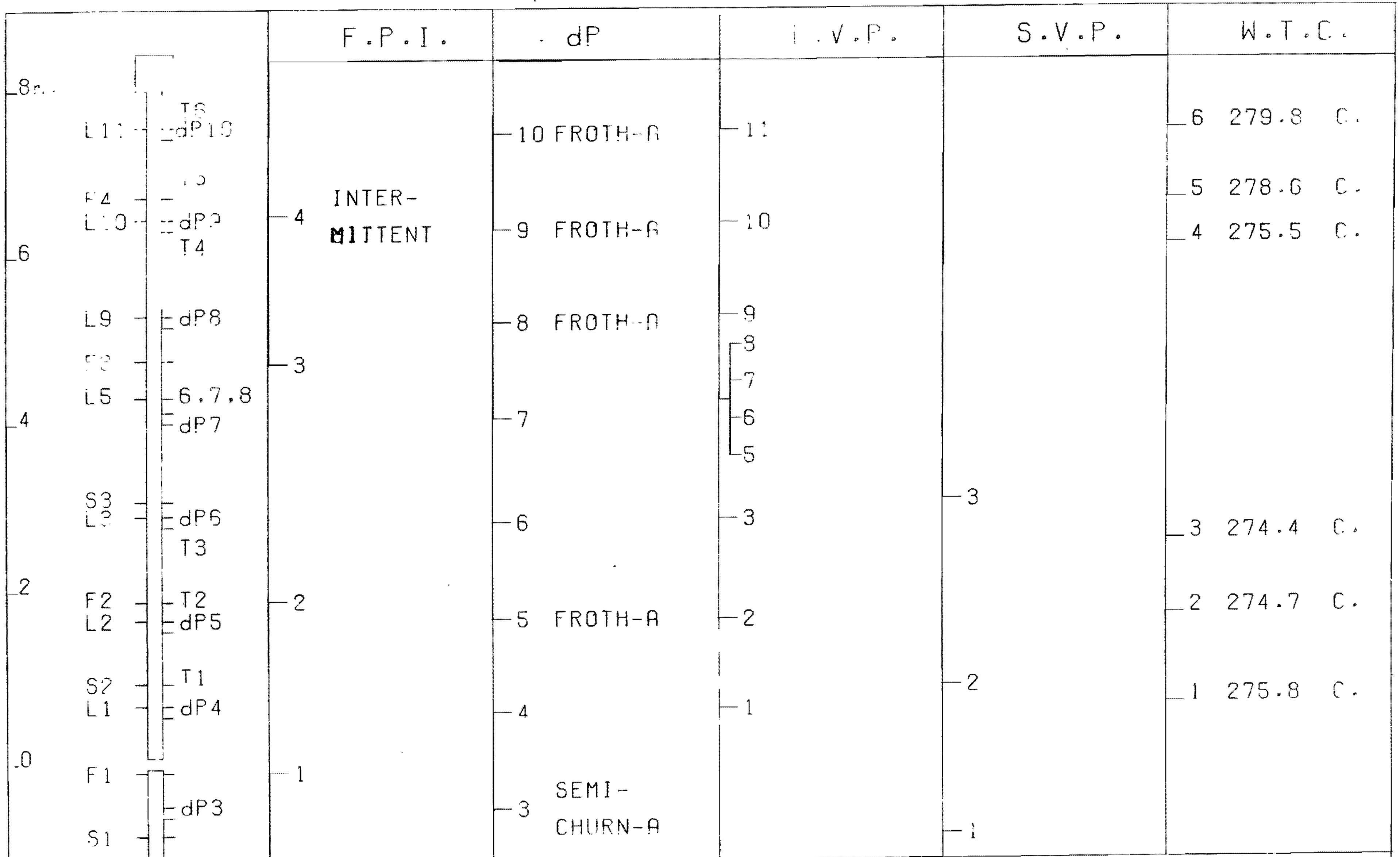

PRESSURE	: 40	BAR
MASS FLOWRATE	: 360	KG/M2.S
HEATING POWER ON TESTSECTION	: 100	k.WATT
HEATING POWER ON PREHEATER	: 200	k.WATT
VOID TESTSECTION INLET	:	%

Fig. 3.18